2012

Analysis of optimal control derivations for aerial defense

Andrew John Friedrichs

Department:

ANALYSIS OF OPTIMAL CONTROL DERIVATIONS FOR AERIAL DEFENSE

by

ANDREW JOHN FRIEDRICHS

A THESIS

Presented to the Graduate Faculty of the

MISSOURI UNIVERSITY OF SCIENCE AND TECHNOLOGY

In Partial Fulfillment of the Requirements for the Degree

MASTER OF SCIENCE IN AEROSPACE ENGINEERING

2012

Approved by

S.N. Balakrishnan, Advisor

Hank Pernicka

Jagannathan Sarangapani

Takeshi Yamasaki

ABSTRACT

Optimal control will be used to derive four guidance laws for the purpose of defending an aircraft from incoming missiles. The dynamics of the defending missile, and the overall engagement are used in these derivations. They are evaluated first in two degrees of freedom, then in six degrees. The guidance objective is to move a defending missile between the aircraft and the attacker. Optimal control is used to derive different commanded accelerations. Utilizing small changes in the cost functions, four applications will be derived. Triangle Guidance is used for inspiration, and initially a direct approach is attempted. In the course of this application a linear weight on the time-to-go, and a hyperbolic on the control weight are used. Three more variations are derived by changing how the dynamics are expressed, and the cost function that is minimized. The results are mixed, with unique problems appearing for each derivation. The final derivation provides a simple expression that proves to be effective. The capture envelope is increased while keeping the control effort low.

ACKNOWLEDGMENTS

Special thanks to my advisor S.N. Balakrishnan for all of his help during the course of my research. Especially for all of the opportunities he has provided including the trip Singapore, and the research fellowship. Thanks to Dr. Pernicka for his help as my undergraduate advisor, for being on my committee, and for his continued advice. Thanks to Dr. Sarangapani for being on my committee, and for the knowledge provided in his classes. Thanks to Dr. Takeshi Yamasaki for all of his help with my research, especially for help with running simulations.

TABLE OF CONTENTS

Page

LIST OF ILUSTRATIONS

NOMENCLATURE

a_c	commanded acceleration (m/s^2)
A-CLOS	Augmented Command to Line of Sight
BA	blue aircraft (cooperative aircraft)
BM	blue missile (defense missile)
d	distance from BM to $LOS_{BA\text{-}RM}$ (m)
γ_i	flight path angle for vehicle *i*, (deg)
H	Hamiltonian
J	performance index
λ_{ij}	LOS angle between *i, j,* (rad)
λ_k	Hamiltonian parameter *k*
LOS*ij*	line-of-sight from the vehicle *j* to the vehicle *i*
OTG	optimal triangle guidance
R	OTG parameter, weight on control
RM	red missile (attacking missile or target)
r_{ij}	and LOS*ij* range, (m)
S	OTG parameter, weight on σ
σ	exterior angle, (rad)
T	final time (s)
t	current time (s)
t_{go}	time to go (s)
TOF	time of flight (s)
u_i	control for body *i*, (m/s^2)
V_c	closing velocity between a BM and a RM (m/s)
V_i	velocity magnitude for body *i* (m/s)
x	state vector

1. INTRODUCTION

Defending aircraft from guided missile attacks is of increasing concern for the Air Force. Current defensives include the use of electronic counter measures, stealth, altitude, defensive maneuvers, decoys, and simply moving faster than the attacking missile. These are mostly passive measures. Stealth works to an extent but does not completely remove an aircraft's radar signature. Defensive maneuvers are restricted by the physical limitations of the aircraft and the pilot. An aircraft moving at subsonic speed has no chance of outrunning a missile. Due to the limitations of using passive countermeasures, a more active approach of destroying an incoming missile is desirable. To this end the concept of aerial defense is introduced. This uses a defensive missile to intercept an attacking missile before it reaches the aircraft. To understand the challenge of intercepting a guided missile with another missile, the history of missile guidance is studied. Missile guidance has been researched, developed and implemented by the Air Force, Navy and the Army. The Navy and the Army are concerned with shooting down aircraft and missiles in order to protect army bases and ships. The development of guided missiles, for the purpose of intercepting an aircraft began after World War II. During World War II, it was clear that a more effective defense was needed to counteract kamikaze attacks. The Navy began development of Lark guided missile in 1944 [1]. After six years of research and development, the Lark missile was the first to successfully intercept an unmanned aircraft. The Lark missile used a widely known control law called proportional navigation (PN). In PN it is desired for the rate of change of the missile's heading to be proportional to the rate of rotation of the LOS from the missile to its target [2]. The commanded acceleration is perpendicular to the LOS from the missile to the target [3]. This commanded acceleration is:

$$n_c = N' V_c \dot{\lambda} \tag{1.1}$$

The commanded acceleration (n_c) is proportional to the closing velocity (V_c) and the rotation of the LOS vector ($\dot{\lambda}$). Consider an engagement scenario where both the missile and the target are moving at the same velocity in one direction, but always moving closer together. This is essentially the goal of PN. For the angle of the LOS to remain constant, both ends must be moving at the same speed perpendicular to the LOS

vector. When this is achieved the missile is on a collision course. This can be seen, in Fig 1.1, by drawing the collision triangle:

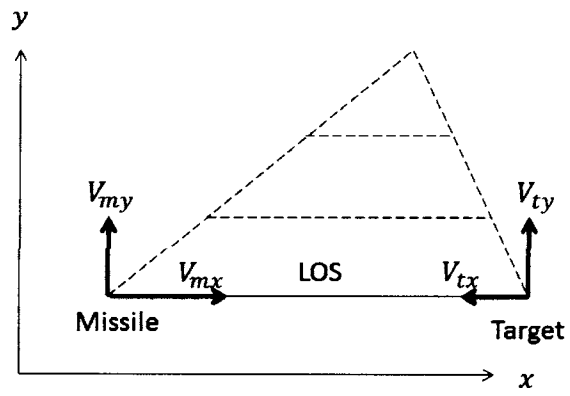

Figure 1.1 Collision Triangle

Simply put the missile and target will be in position in the $\hat{y}$ direction, including when their relative distance in the $\hat{x}$ direction reaches zero, resulting in a collision. PN counteracts the rotation of the LOS vector, changing the direction of the missile's velocity so that its component perpendicular to the LOS matches the target's perpendicular velocity. PN is simple yet effective. However, it does not take into account gravity, or any maneuvers the target may employ. There is also no optimization of the commanded acceleration. A variation of PN called augmented proportional navigation (APN), contains an extra term to compensate for a maneuvering target. The commanded acceleration is changed to

$$n_c = N' V_c \dot{\lambda} + \frac{N' n_T}{2} \tag{1.2}$$

One obvious problem is that a reliable estimate of the target's acceleration (n_T) is required. One advantage to PN is that the closing velocity and LOS rate are relatively

easy to measure. The target's acceleration can be found from this information; however it is not directly measured. It is measured by taking previous information and creating an estimate based on the change of the target's velocity.

The first USAF air-to-air intercept was achieved during the Vietnam War. This was done by an F-4 Phantom using a AIM-9 Sidewinder [4]. This success was soon shadowed by another F-4 Phantom that was shot down by an enemy SAM. The F-4 Phantom was also the first United States aircraft to be shot down by an enemy air-to-air missile. These events highlight the importance of protecting aircraft from missiles. The fact that aircraft continue to be shot down, shows that the current measures are not completely effective.

The most widely known missile defense system is the Patriot missile. It was the first missile defense system to be proved in combat. In the early 90's the Patriot missile was used during the Gulf War to intercept Scud missiles. Its effectiveness was the topic of some debate. Success is typically defined as the percentage of engaged missiles that do not hit their target. Accuracy is typically defined as the percentage of engaged missiles that are destroyed. For the Patriot missile system it was sufficient to merely deflect an incoming missile, so that it did not hit its target. One idea to improve the intercept of ASM with a SAM is the concept of the Earliest Intercept Line (EIL). The specific goal of EIL is to improve missile-to-missile single shot kill probability [6]. For the Navy and the Army, the concept of area defense is important. This is deploying a missile system so that it can protect a military outpost, or for one ship to protect several ships. Robb uses the EIL to develop a concept of reachability in area defense. This is done by calculating the earliest possible intercept point given the missile's current position and heading. These concepts are important to keep in mind.

The specific problem that will be addressed in this thesis will be that of defending an aircraft from an incoming missile. The goal will be to have a missile, the blue missile (BM), intercept an attacking missile, the red missile (RM), before it hits the aircraft (BA). The engagement can be illustrated by drawing a triangle with one of the vehicles at each point. This is shown in Fig 1.2.

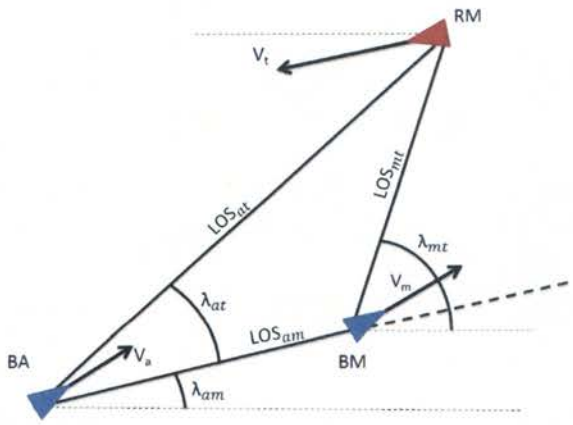

Figure 1.2 Engagement Geometry

Rusnak [8] wrote about applying differential game theory to the problem of defending an aircraft with a missile. The problem is broken into two parts: first, the attacking missile and the target, and second, the defender intercepting the attacker. It is assumed that the target is evading the attacker while the defender is intercepting the attacker. To achieve this Rusnak uses optimal control to minimize the distance between the defender and the attacker, while maximizing the distance between the attacker and the target.

The geometry of the engagement leads to a common objective for many control schemes. The goal is to move the BM between the BA and RM. It is reasonable to assume that the RM is on a collision course with the BA. If the RM is not on a collision course there is not need to protect the aircraft. The benefit of the RM trying to intercept the BA, is that the LOS_{at} is always decreasing. This means that if the BM is between the BA and RM, the RM will eventually hit the BM. This engagement is considered by Boyell [7], which considers the dynamics in defending a moving target. Boyell calculates the optimal launch angle for a defending missile to achieve a minimum time to intercept. Missile intercept guidance is typically broken into two parts, mid-course and terminal. This partially comes from the hardware limitations of the missiles used. Whether using infrared or radar, most missiles are not able to track a target when launched. They use

information from an external radar source during mid-course guidance. Terminal guidance is the last stage of the intercept, when the missile has locked on to the target. A new problem comes when using an aircraft to fire a missile. Missiles are typically fired straight forward from an aircraft. If a missile is fired at an aircraft with a significant heading error, the intercept missile would also have a significant heading error. The infrared or radar used by a missile may not be able to see the incoming missile, until this heading error is reduced. This idea of moving the BM to LOS_{at} has lead to many LOS guidance laws called command to line of sight (CLOS). Perelman [9] deals with dynamics in 2D, and specifically deals with testing the effects of a maneuvering aircraft on a defending missile's intercept. A common assumption of constant velocities is also used. In PN, when a missile wants to intercept a target, the rotation of the LOS from missile to target is reduced. Remember that the goal is to keep the LOS constant and reduce the range. In this LOS guidance law the goal is for all three of the LOS vectors to rotate at the same rate. This makes sense because if the BM stays on LOS_{at}, the LOS vectors to and from the BM must rotate at the same rate as LOS_{at}. The major focus seemed to be more on what the aircraft can do to make the attacking missile work harder than the defending missile. A slightly different approach to the problem was explored by Rantoo [10]. Rantoo also deals with dynamics in 2D. The aircraft is used by providing information to the BM about the RM. It is shown is that if the aircraft provides a more accurate estimate, the defender expends less effort.

A guidance law that does directly use the geometry of the aerial defense problem is triangle guidance (TG) [11]. This guidance law takes a unique approach to the problem. It focuses on the idea of collapsing the engagement triangle. This is done by using the exterior angle σ, and can be calculated using the two LOS angles to and from the BM. The exterior angle is seen in Fig 1.3.

$$\sigma = \lambda_{mt} - \lambda_{am} \tag{1.3}$$

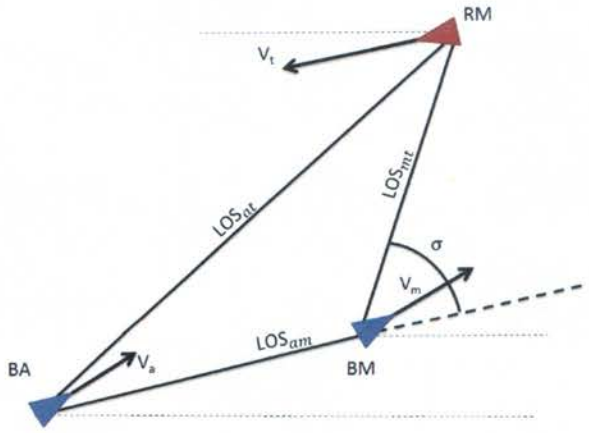

Figure 1.3 Exterior Angle σ

The control law proposed was:

$$a_c = V_c(N\sigma + N_d\dot{\sigma}) \tag{1.4}$$

It was found that using a commanded control proportional only to the current value of σ preforms poorly. It is desirable for the BM to move between the BA and RM, and stay there. Using only the current value of the angle, the BM tends to overshoot and move from one side of LOS_{at} to the other side. The advantage to TG is that it used an approach that directly uses the geometry of the engagement. It does not require the aircraft to provide additional information. In TG the commanded acceleration a_c is perpendicular to LOS_{at}. In theory the focus is on moving to the LOS rather than moving down it. However, in application we have little control over the BM's velocity. Control surfaces on a missile are used to rotate the body axis. In most simulations the body axis is assumed to coincide with the velocity vector. This means that the applied acceleration will be different than the commanded acceleration. In TG the applied acceleration perpendicular to the velocity is increased so that its component perpendicular to LOS_{at} is the magnitude of the commanded acceleration. The guidance laws discussed provide several important concepts to keep in mind. A common concept used in guidance laws is to include the aircraft by having it measure the acceleration of the incoming missile. This

is most notably done by Shima who does propose using information from both the defending missile and the aircraft's sensors to create a perfect estimation of the incoming missile's acceleration. Furthermore, he proposes estimating the guidance law used by the attacker [12]. This paper will focus on deriving an optimal control guidance law using a geometric approach similar to what is seen in TG.

2. OPTIMAL CONTROL

The goal of this thesis is to apply optimal control to the aerial defense problem. Before this can be done a general form of the optimal control will be derived. First, a performance index is chosen of the form

$$J = \varphi\big(x(T)\big) + \int_{t_0}^{T} L(x,u)dt \tag{2.1}$$

subject to the system dynamics

$$\dot{x} = f(x,u) \tag{2.2}$$

with initial conditions

$$x(t_0) = x_0 \tag{2.3}$$

The Hamiltonian is formed from the performance index and the system model

$$H(x,u,\lambda) = L(x,u) + \lambda^T f(x,u) \tag{2.4}$$

Augment the performance index with the Hamiltonian

$$J' = \varphi\big(x(T)\big) + \int_{t_0}^{T} \{H(x,u,\lambda) - \lambda^T f(x,u)\}dt \tag{2.5}$$

To find the minimum of the performance index taking the first variation

$$\delta J' = \varphi_x \delta x_f + \int_{t_0}^{T} \{H_x \tilde{\delta} x + H_u \tilde{\delta} u + H_\lambda \tilde{\delta}\lambda - \tilde{\delta}\lambda^T \dot{x} - \lambda^T \tilde{\delta}\dot{x}\}dt + \cdots \{(H(x,u,\lambda) - \lambda^T \dot{x})\delta t\}_{t_0}^{T} \tag{2.6}$$

Consider that the fixed variation $\tilde{\delta}x$ is related to the time free variation δx

$$\delta x = \tilde{\delta} x + \dot{x}\delta t \tag{2.7}$$

Using the fact that $H_\lambda = f(x,u)$ leads to

$$H_\lambda \tilde{\delta}\lambda - \tilde{\delta}\lambda^T \dot{x} = (f(x,u) - \dot{x})\tilde{\delta}\lambda = 0 \tag{2.8}$$

and

$$\delta J' = \varphi_x \delta x_f + \int_{t_0}^{T} \{H_x \tilde{\delta}x + H_u \tilde{\delta}u\} dt - \int_{t_0}^{T} \{\lambda^T \tilde{\delta}\dot{x}\} dt + \{H(x,u,\lambda) - \lambda^T \dot{x}\}_{t_0}^{T} \tag{2.9}$$

Expanding the third term using integration by parts yields

$$\int_{t_0}^{T} \{\lambda^T \tilde{\delta}\dot{x}\} dt = \{\lambda^T \tilde{\delta}x\}_{t_0}^{T} - \int_{t_0}^{T} \{\dot{\lambda}^T \tilde{\delta}x\} dt \tag{2.10}$$

$$\{\lambda^T \tilde{\delta}x\}_{t_0}^{T} = \{\lambda^T (\delta x - \dot{x}\delta t)\}_{t_0}^{T} = \{\lambda^T \delta x\}_{t_0}^{T} - \{\lambda^T \dot{x}\delta t\}_{t_0}^{T} \tag{2.11}$$

Considering the initial time, final time and state are known

$$\delta x_{t_0} = \delta t_{t_0} = \delta t_f = 0 \tag{2.12}$$

$$\int_{t_0}^{T} \{\lambda^T \tilde{\delta}\dot{x}\} dt = \lambda_f^T \delta x_f - \int_{t_0}^{T} \{\dot{\lambda}^T \tilde{\delta}x\} dt \tag{2.13}$$

Using (7) and (10) in (9)

$$\delta J' = \varphi_x \delta x_f - \lambda_f^T \delta x_f + \int_{t_0}^{T} \{H_x \tilde{\delta}x + H_u \tilde{\delta}u + \dot{\lambda}^T \tilde{\delta}x\} dt \tag{2.14}$$

Combining like terms

$$\delta J' = (\varphi_x - \lambda_f^T)\delta x_f + \int_{t_0}^{T} \{(H_x + \dot{\lambda}^T)\tilde{\delta}x + H_u \tilde{\delta}u\} dt \tag{2.15}$$

Consider that the Lagrange multipliers λ can be chosen to eliminate the dependent variations. This leads to the costate equation

$$\dot{\lambda}^T = -H_x = -\frac{\partial H}{\partial x} \tag{2.16}$$

and boundary condition

$$\lambda_f^T = \varphi_x = \frac{\partial \varphi}{\partial x} \tag{2.17}$$

This leaves only

$$\delta J' = \int_{t_0}^{T} \{H_u \tilde{\delta} u\} dt \tag{2.18}$$

To ensure the cost function is minimized, the first variation must be zero. This leads to the necessary condition

$$H_u = \frac{\partial H}{\partial u} = 0 \tag{2.19}$$

3. SYSTEM DYNAMICS

Consider the dynamics of a missile. The rocket motor does not have a throttle so there is no control over the thrust of the missile. The control comes from the fins of the rocket, which are used to rotate the missile. This can be shown as a force perpendicular to the body axis. It is assumed that the velocity is in the same direction as the body axis. The missile will go through a thrusting faze and a coasting phase. During the thrusting phase, the velocity will increase rapidly, but during the coasting phase, drag will slowly decrease the velocity. For 2D simulations the velocity magnitude of the both defending missile and the incoming missile's is assumed to be constant along the body axis seen in Fig 3.1. The aircraft is moving with a constant velocity and direction. A state space representation of the system is needed to apply optimal control. How the system dynamics, derived from the forces seen in Fig 3.2, are modeled has a large impact on applying optimal control. The coordinate system that is used changes how the dynamics are expressed and thus how the derivatives in optimal work out.

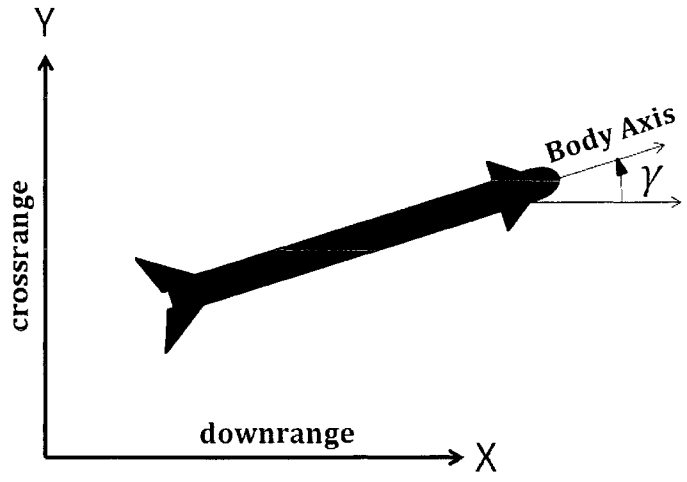

Figure 3.1 Flight Path Angle

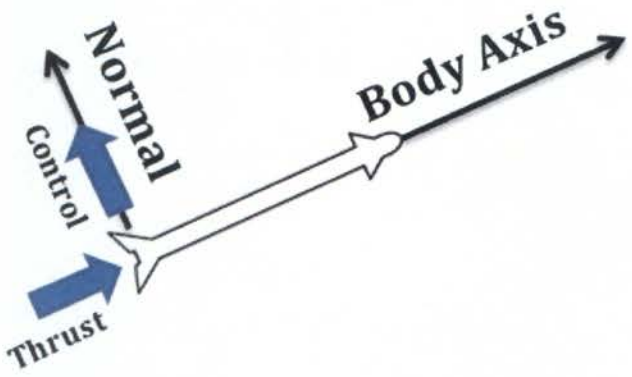

Figure 3.2 Forces

Each application needs a state space representation of the dynamics in Fig 3.3 and an expression for the position and velocity of each body.

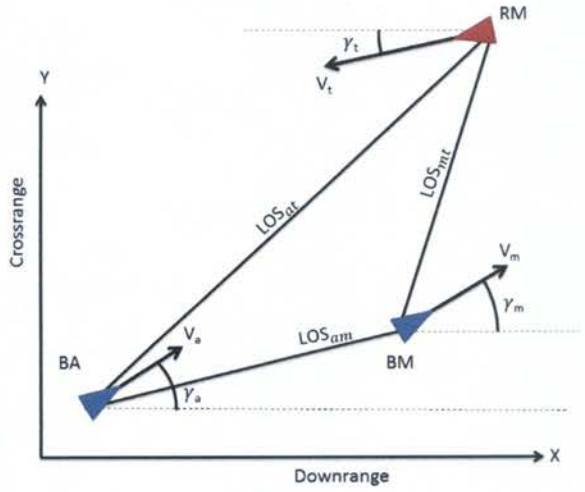

Figure 3.3 Engagement

The simplest way to do this is to use the inertial position and velocity of each body. A similar method is to use the inertial position and flight path angle FPA for each body. This assumes the velocities are constant. A third way used is to express the dynamics in a different coordinate system. These differences lead to large changes in the final control expression.

4. APPLICATIONS

Optimal control was applied to this problem in several different ways. They all center on how the state dynamics are expressed, and which cost function is chosen.

$$J = \varphi\big(x(T)\big) + \int_{t_0}^{T} L(x,u)dt \tag{4.1}$$

$$\dot{x} = f(x,u) \tag{4.2}$$

4.1. APPLICATION I

Triangle guidance centered on reducing the exterior angle σ. This was the first method considered. To this end the following cost function was chosen

$$J = \frac{1}{2}S\sigma^2 + \int_{t_0}^{T} \frac{1}{2}Ru_m^2 dt \tag{4.3}$$

This would attempt to minimize the control effort used while reducing σ. This leads to

$$H(x,u,\lambda) = \frac{1}{2}Ru_m^2 + \lambda^T f(x,u) \tag{4.4}$$

$$\dot{\lambda}^T = -\lambda^T \frac{\partial}{\partial x} f(x,u) \tag{4.5}$$

$$\frac{\partial H}{\partial u} = Ru_m + \lambda^T \frac{\partial}{\partial u} f(x,u) \tag{4.6}$$

$$\lambda_f^T = \frac{\partial \varphi}{\partial x}\bigg|_{t=T} = \frac{\partial \frac{1}{2}S\sigma^2}{\partial x}\bigg|_{t=T} \tag{4.7}$$

The optimal control equations are subject to the system dynamics

$$\dot{x} = f(x,u) \tag{4.8}$$

There are many different ways to express the system dynamics. At first it was desired to express them in the form

$$\dot{\sigma} = f(\sigma,u) \tag{4.9}$$

If $\dot{\sigma}$ can be expressed as an explicit function of σ, then the equations seen in (4.4) through (4.7) can be easily evaluated. However, no such function was found. Consider that σ is not dependent on the velocity of the vehicles. If the velocity of the BM is rotated, it will not change the value of σ, but it could cause it to rotate faster or slower. In the end, a simpler set of dynamics was chosen

$$x = [BA_x\ BA_y\ BM_x\ BM_y\ RM_x\ RM_y\ \gamma_A\ \gamma_m\ \gamma_t]^T \tag{4.10}$$

$$\dot{x} = [V_a\cos(\gamma_A)\ V_a\sin(\gamma_A)\ V_m\cos(\gamma_m)\ V_m\sin(\gamma_m)\ V_t\cos(\gamma_t)\ V_t\cos(\gamma_t)\ \frac{\dot{\gamma}_a}{V_a}\ \frac{u_m}{V_m}\ \frac{\dot{\gamma}_t}{V_t}]^T \tag{4.11}$$

These dynamics assume that each vehicle is moving at a constant velocity. The FPA is used because, in application, a missile's velocity is controlled by the rocket motor. We have no control over the magnitude of the velocity, but the direction can be controlled. To this end the dynamics are expressed in terms of the position and FPA of each body.

Taking the derivative of the Hamiltonian with respect to λ gives the state equation:

$$\frac{\partial H}{\partial \lambda} = \dot{x} = [V_a\cos(\gamma_A)\ V_a\sin(\gamma_A)\ V_m\cos(\gamma_m)\ V_m\sin(\gamma_m)\ V_t\cos(\gamma_t)\ V_t\cos(\gamma_t)\ \frac{\dot{\gamma}_a}{V_a}\ \frac{u_m}{V_m}\ \frac{\dot{\gamma}_t}{V_t}]^T \tag{4.12}$$

The derivative with respect to u_m produces the stationary condition:

$$\frac{\partial H}{\partial u} = Ru_m + \frac{\lambda_8}{V_m} = 0 \tag{4.13}$$

$$u_m = -R^{-1}\frac{\lambda_8}{V_m} \tag{4.14}$$

The λ_8 term corresponds to the control for the BM. Expanding the costate equation, $\lambda_1$through λ_6 are constant because the derivative of the state vector is not a function of the current position. The velocity of each vehicle does not depend on its current position. The derivative of the λ vector is:

$$\dot{\lambda} = -\frac{\partial}{\partial x}[V_a \cos(\gamma_A)\ V_a \sin(\gamma_A)\ V_m \cos(\gamma_m)\ V_m \sin(\gamma_m)\ V_t \cos(\gamma_t)\ V_t \cos(\gamma_t)\ \frac{\dot{\gamma}_a}{V_a}\ \frac{u_m}{V_m}\ \frac{\dot{\gamma}_t}{V_t}]^T \lambda^T \quad (4.15)$$

$$[\dot{\lambda}_1 \quad \dot{\lambda}_2 \quad \dot{\lambda}_3 \quad \dot{\lambda}_4 \quad \dot{\lambda}_5 \quad \dot{\lambda}_6]^T = [0 \quad 0 \quad 0 \quad 0 \quad 0 \quad 0]^T \quad (4.16)$$

The last three differential equations $\dot{\lambda}_7, \dot{\lambda}_8$, and $\dot{\lambda}_9$ are a function of the first six, the velocity of each body, and their flight path angles.

$$\dot{\lambda}_7 = -\frac{\partial \dot{x}}{\partial \gamma_A} = -V_a \sin(\gamma_A)\,\lambda_1 + V_a \cos(\gamma_A)\,\lambda_2 \quad (4.17)$$

$$\dot{\lambda}_8 = -\frac{\partial \dot{x}}{\partial \gamma_m} = -V_m \sin(\gamma_m)\,\lambda_3 + V_m \cos(\gamma_m)\,\lambda_4 \quad (4.18)$$

$$\dot{\lambda}_9 = -\frac{\partial \dot{x}}{\partial \gamma_t} = -V_t \sin(\gamma_t)\,\lambda_5 + V_t \cos(\gamma_t)\,\lambda_6 \quad (4.19)$$

These equations can be written in terms of derivatives of the positions of each of the bodies:

$$\dot{\lambda}_7 = -B\dot{A}_y\lambda_1 + B\dot{A}_x\lambda_2 \quad (4.20)$$

$$\dot{\lambda}_8 = -B\dot{M}_y\lambda_3 + B\dot{M}_x\lambda_4 \quad (4.21)$$

$$\dot{\lambda}_9 = -R\dot{M}_y\lambda_5 + R\dot{M}_x\lambda_6 \quad (4.22)$$

These equations can be integrated with λ_1-λ_6 as constants. This is a very important step in optimal control. In many optimal control problems, the derivative of the state and the derivative of the λ vector must be solved simultaneously. This can be difficult in the best of cases and not possible in others. Because every element in the λ vector is constant or a function of the state derivative, these equations can be easily integrated.

$$\lambda_7 = -BA_y\lambda_1 + BA_x\lambda_2 + C_1 \quad (4.23)$$

$$\lambda_8 = -BM_y\lambda_3 + BM_x\lambda_4 + C_2 \quad (4.24)$$

$$\lambda_9 = -RM_y\lambda_5 + RM_x\lambda_6 + C_3 \quad (4.25)$$

The C_1, C_2, and C_3 terms are constants of integration and can be solved using the boundary condition from optimal control.

$$(\varphi_x - \lambda)|_T dx(T) = 0 \tag{4.26}$$

$$\lambda_f = \frac{\partial \varphi_f^T}{\partial x} \tag{4.27}$$

This gives the values for λ at the final time in terms of the derivative of the final state constraint with respect to the state vector. From equation (4.3), the final state constraint is:

$$\varphi(x(T), T) = \frac{1}{2} S\big(\sigma(T)\big)^2 \tag{4.28}$$

The angle σ can be calculated using the two LOS angles:

$$\lambda_{Am} = \tan^{-1}(\beta_1) \qquad \lambda_{mt} = \tan^{-1}(\beta_2) \tag{4.29}$$

$$\beta_1 = \frac{BM_y - BA_y}{BM_x - BA_x} \qquad \beta_2 = \frac{RM_y - BM_y}{RM_x - BM_x} \tag{4.30}$$

The derivatives of $\varphi(x(T), T)$ with respect to the state for λ_1 through λ_6 are:

$$\lambda_1 = \frac{\partial \varphi_f^T}{\partial BA_x} = S\sigma \frac{\beta_1}{(1+\beta_1^2)(BM_x - BA_x)}\bigg|_T \tag{4.31}$$

$$\lambda_2 = \frac{\partial \varphi_f^T}{\partial BA_y} = -S\sigma \frac{1}{(1+\beta_1^2)(BM_x - BA_x)}\bigg|_T \tag{4.32}$$

$$\lambda_3 = \frac{\partial \varphi_f^T}{\partial BM_x} = S\sigma \left\{\frac{\beta_1}{(1+\beta_1^2)(BM_x - BA_x)} + \frac{\beta_2}{(1+\beta_2^2)(RM_x - BM_x)}\right\}\bigg|_T \tag{4.33}$$

$$\lambda_4 = \frac{\partial \varphi_f^T}{\partial BM_y} = -S\sigma \left\{\frac{1}{(1+\beta_1^2)(BM_x - BA_x)} + \frac{1}{(1+\beta_2^2)(RM_x - BM_x)}\right\}\bigg|_T \tag{4.34}$$

$$\lambda_5 = \frac{\partial \varphi_f^T}{\partial RM_x} = S\sigma \frac{\beta_2}{(1+\beta_2^2)(RM_x - BM_x)}\bigg|_T \tag{4.35}$$

$$\lambda_6 = \frac{\partial \varphi_f^T}{\partial RM_y} = -S\sigma \frac{1}{(1+\beta_2^2)(RM_x - BM_x)}\bigg|_T \tag{4.36}$$

From equation (4.14) only λ_8 is needed in the control equation. The λ_7 and λ_9 terms are not directly needed, and do not show up in any of the other derivatives. Only two of the first six derivatives, λ_3 and λ_4, are needed for control. These two elements are only a function of the final state and can be reduced to:

$$\lambda_3 = \frac{\partial \varphi_f^T}{\partial BM_x} = S\sigma \left\{ \frac{(BM_y - BA_y)}{R_{ma}^2} + \frac{(RM_y - BM_y)}{R_{tm}^2} \right\} \Big|_T \tag{4.37}$$

$$\lambda_4 = \frac{\partial \varphi_f^T}{\partial BM_y} = -S\sigma \left\{ \frac{(BM_x - BA_x)}{R_{ma}^2} + \frac{(RM_x - BM_x)}{R_{tm}^2} \right\} \Big|_T \tag{4.38}$$

The FPA of the missile is not needed to calculate σ at the final time. The condition $\varphi(x(T), T)$ is a function of the final position only makes the value of λ_8 at the final time zero.

$$\lambda_{8f} = \frac{\partial \varphi_f^T}{\partial \alpha_m} = 0 \tag{4.39}$$

All of the information needed to calculate the desired control is available, except the positions of each body at the final time. The final positions are calculated assuming constant velocities in constant direction. This prediction will become more accurate as the BM approaches the RM, and is similar to how the zero effort miss ZEM is calculated. If both of the missiles do not maneuver their closest point is the ZEM. The only difference is that t_{go} is used instead of whatever time takes the missiles to reach their closest point. The t_{go} term is easier to calculate. Therefore the state can be calculated at the final time:

$$x(T) = \dot{x}(t) t_{go} + x(t) \tag{4.40}$$

The C_2 term in λ_8 can now be calculated using the information at the final time:

$$\lambda_8 = -BM_y \lambda_3 + BM_x \lambda_4 + C_2 \tag{4.41}$$

$$C_2 = BM_{yf} \lambda_3 - BM_{xf} \lambda_4 \tag{4.42}$$

$$\lambda_8 = -(BM_y - BM_{yf}) \lambda_3 + (BM_x - BM_{xf}) \lambda_4 \tag{4.43}$$

$$\lambda_8 = -(BM_y - \dot{BM}_y t_{go} - BM_y)\lambda_3 + (BM_x - \dot{BM}_x t_{go} - BM_x)\lambda_4 \quad (4.44)$$

$$\lambda_8 = V_m \cos(\gamma_m)\, t_{go}\lambda_4 - V_m \sin(\gamma_m)\, t_{go}\lambda_3 \quad (4.45)$$

$$u_m = -R^{-1}\frac{\lambda_8}{V_m} \quad (4.46)$$

This leads to the control as:

$$u_m = R^{-1}\{\sin(\gamma_m)\, t_{go}\lambda_3 - \cos(\gamma_m)\, t_{go}\lambda_4\} \quad (4.47)$$

Equation (3.47) provides the magnitude of the control for the BM. The direction, from the dynamics, is perpendicular to the velocity of the missile. λ_3 and λ_4 are calculated from equations (4.37) and (4.38). In this guidance law it is desired for σ to go to zero before the BM is predicted to reach the RM. This is done by scaling t_{go}:

$$t_{go} = 0.70\frac{r_{mt}}{\dot{r}_{mt}} \quad (4.48)$$

The simulation used to test optimal triangle guidance OTG has the RM starting 10km downrange and 16.5km cross range. Both the BM and the RM are traveling at a constant velocity of 800 m/s. The aircraft is traveling at 250 m/s without changing direction. The weight on σ (S) is 1 while the weight on control (R) varies from $8\text{x}10^{-6}$ to $8\text{x}10^{-9}$ using a hyperbolic tangent function. The RM is using PN to chase the aircraft. The target's acceleration is not required in OTG, but it is used in this simulation. When it is not used, the miss distance is larger, but is still below 1/10 of a meter. The trajectory is shown in Fig. 4.1:

In this simulation the BM misses the RM by 0.034 m. Fig. 4.2 shows the acceleration demanded by OTG. The value of u_m is initially high, because the control is rotating the trajectory of the BM to intercept the RM. This can be seen in the LOS rate and closing velocity. The LOS between the BM and RM is rotated so that their velocities are pointed towards each other, causing the closing velocity to increase.

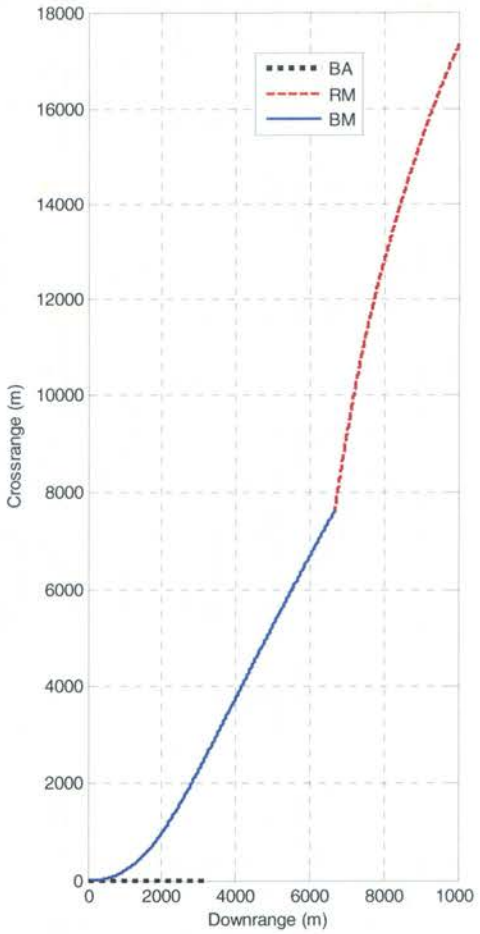

Figure 4.1 Trajectory.

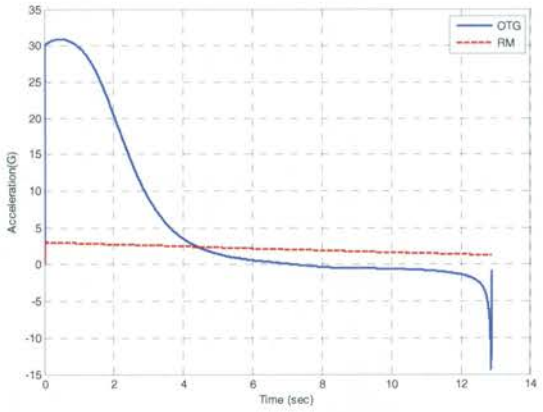

Figure 4.2 Commanded Control.

The weight on control in Fig 4.3 is decreased as the BM approaches the RM, causing the guidance law to demand more acceleration to intercept the RM. The goal of the OTG formulation is met as seen in the plot of σ in Fig. 4.4. The value for σ increases slightly at the beginning of the simulation. This is due to system dynamics. It can be seen in the plot of $\dot{\sigma}$ that σ is increasing at the beginning of the simulation, due to initial conditions.

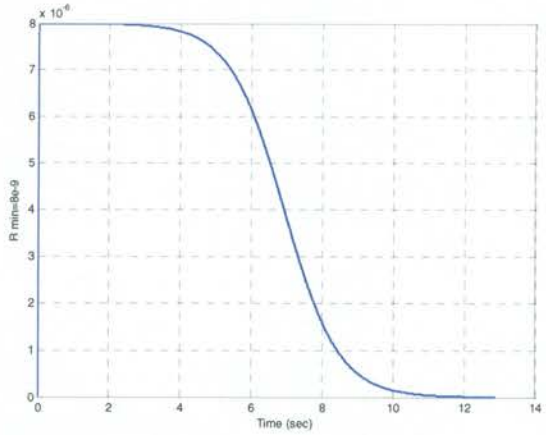

Figure 4.3 Weight on Control (R).

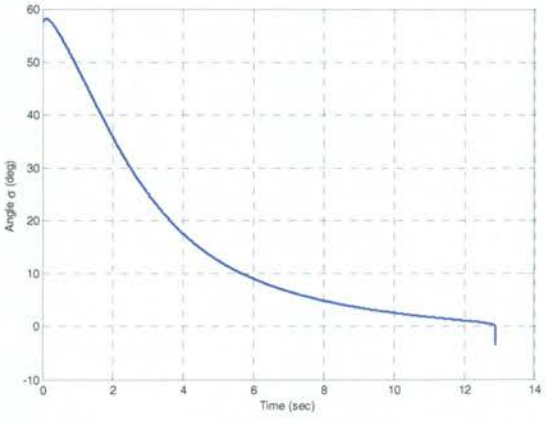

Figure 4.4 Sigma.

Sigma decreases exponentially, which is desirable, but in the last time steps of 2ms the value of σ dips below zero. Fig. 4.5 shows $\dot{\sigma}$. The steep decrease in σ can be seen in the last second in Fig. 4.4. Despite this the BM comes within three hundredths of a meter of the RM.

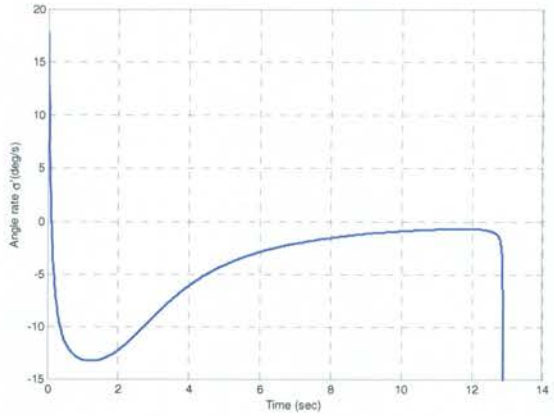

Figure 4.5 Sigma Dot

Additional simulations were run with the RM having slightly different initial conditions. These can be seen in Fig. 4.6 Three were placed above the x axis and three below. The RM was placed from 67^0 above to 67^0 below the aircraft. The miss distances are slightly larger, because the tuning parameters were not changed from the previous results shown. When the RM is placed higher or lower, the tuning parameters must be changed slightly.

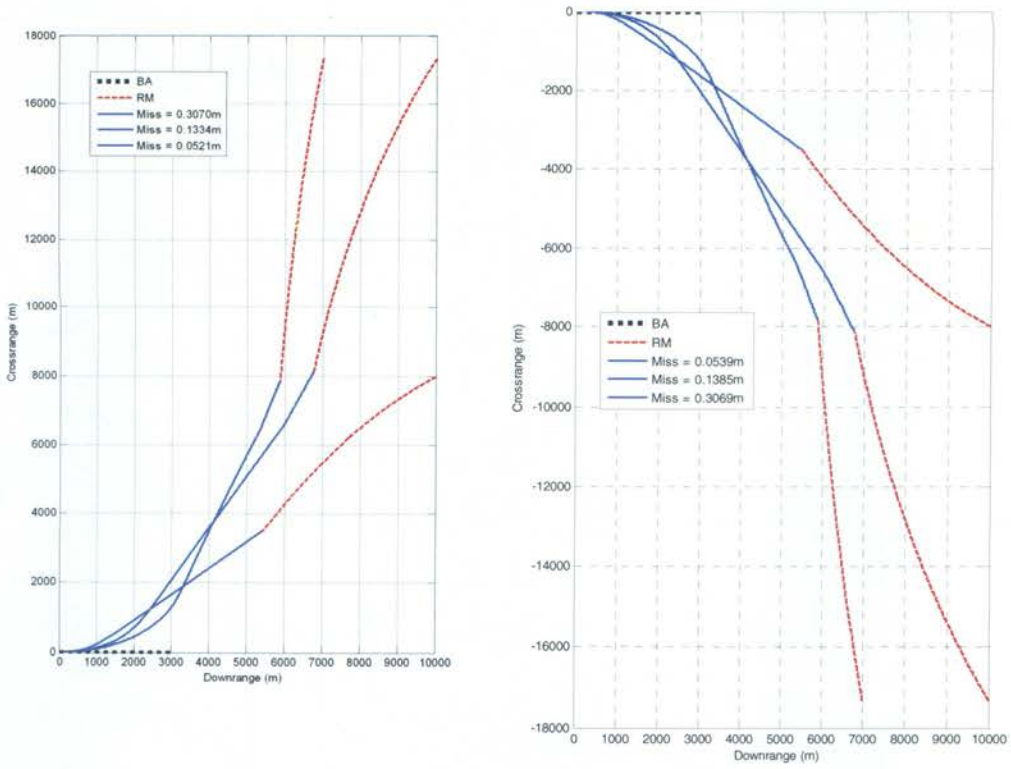

Figure 4.6 Additional Trajectories.

Though this derivation was successful in 2D, it did not perform well in 3D. The state dynamics were expressed in a similar manner, adding a z component to the position for each vehicle and a second FPA (ψ) corresponding to the component of the velocity out of the x-y plane. This led to a second control term, which is to be expected.

$$\bar{X} = [\overline{BA} \;\; \overline{BM} \;\; \overline{RM} \;\; \gamma_A \;\; \psi_A \;\; \gamma_M \;\; \psi_M \;\; \gamma_T \;\; \psi_T] \tag{4.49}$$

$$\overline{BM} = \begin{bmatrix} BM_x & BM_y & BM_z \end{bmatrix} \tag{4.50}$$

$$\dot{\bar{X}} = f(x,u) = \left[\bar{V}_A \; \bar{V}_M \; \bar{V}_T \;\; \dot{\gamma}_A \; \dot{\psi}_A \; \frac{U_{M\gamma}}{V_m} \; \frac{U_{M\psi}}{V_m} \; \dot{\gamma}_T \; \dot{\psi}_T\right] \tag{4.51}$$

$$\bar{\mathrm{V}}_\mathrm{m} = \mathrm{V_m}\cos(\psi)\sin(\gamma)\,\hat{\mathrm{x}} + \mathrm{V_m}\cos(\psi)\cos(\gamma)\,\hat{\mathrm{y}} + \mathrm{V_m}\sin(\psi)\,\hat{\mathrm{z}} \tag{4.52}$$

The problem comes when trying to solve the costate equation, specifically when solving for the derivative of the Hamiltonian with respect to ψ.

$$\dot{\lambda}_{13} = -\frac{\partial H}{\partial \psi} = -\frac{\partial}{\partial \psi}\left(V_m \cos(\psi)\cos(\gamma)\lambda_4 + V_m \cos(\psi)\sin(\gamma)\lambda_5 - V_m \sin(\psi)\,\lambda_6\right) \quad (4.53)$$

$$\dot{\lambda}_{13} = \left(V_m \sin(\psi)\cos(\gamma)\lambda_4 + V_m \sin(\psi)\sin(\gamma)\lambda_5 + V_m \cos(\psi)\,\lambda_6\right) \quad (4.54)$$

Unlike the 2D derivation, this equation cannot be easily integrated. This means that an analytical solution for λ_{13} cannot be found. Another idea that was attempted was that of using a coordinate frame attached to the plane made by the three bodies. The coordinate frame in Fig4.7 has one axis along the LOS from the BA to the BM, a second perpendicular to the first in the σ-plane, and a third perpendicular to the plane.

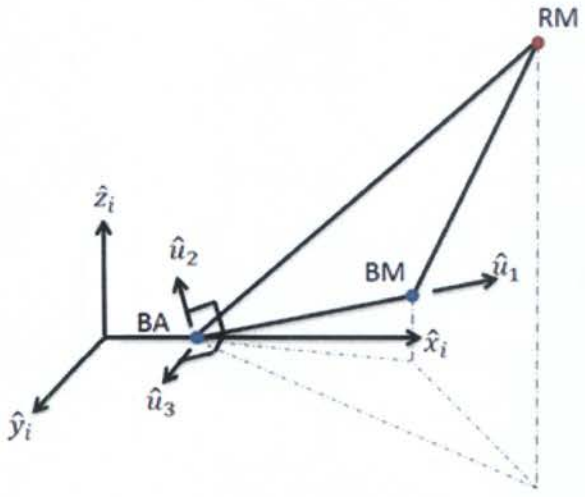

Figure 4.7 σ-plane Coordinate System

The idea was to force the 2D solution into this rotating coordinate frame. If optimal control can reduce the engagement triangle in 2D, then that solution can rotate with the σ-plane. Ignoring the rotation ignores dynamics of the system. Specifically, velocities out of the plane would be ignored.

Sigma decreases exponentially, which is desirable, but in the last time steps of 2ms the value of σ dips below zero. Fig. 4.5 shows $\dot{\sigma}$. The steep decrease in σ can be seen in the last second in Fig. 4.4. Despite this the BM comes within three hundredths of a meter of the RM.

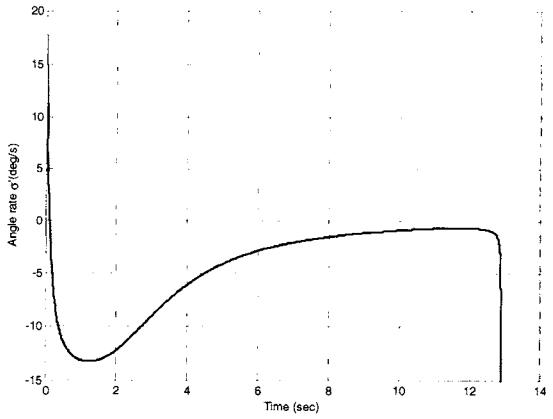

Figure 4.5 Sigma Dot

Additional simulations were run with the RM having slightly different initial conditions. These can be seen in Fig. 4.6 Three were placed above the x axis and three below. The RM was placed from 67^0 above to 67^0 below the aircraft. The miss distances are slightly larger, because the tuning parameters were not changed from the previous results shown. When the RM is placed higher or lower, the tuning parameters must be changed slightly.

4.2. APPLICATION II

Similar to previous derivations the state chosen for this new idea is simply the position and velocity of each vehicle. The state dynamics are easily calculated:

$$\bar{x} = [\overline{BA} \quad \overline{BM} \quad \overline{RM} \quad \bar{V}_a \quad \bar{V}_m \quad \bar{V}_t]^T \tag{4.55}$$

$$\dot{\bar{x}} = [\bar{V}_a \quad \bar{V}_m \quad \bar{V}_t \quad \bar{A}_a \quad \bar{A}_m \quad \bar{A}_t]^T \tag{4.56}$$

The acceleration for the missile is described using the inertial x-y frame. The original OTG derivation assumes the control direction to be perpendicular to velocity which also assumes there is no direct control of the missile's velocity magnitude. These assumptions will be addressed later in simulations. Using the inertial acceleration simplifies the optimal control equations.

$$\bar{A}_m = u_x\hat{x} + u_y\hat{y} \tag{4.57}$$

The cost function and Hamiltonian is the same as used previously

$$J = \varphi + \int_{t_o}^{T} \frac{R}{2}\left(u_x^2 + u_y^2\right) dt \tag{4.58}$$

$$H = \frac{R}{2}\left(u_x^2 + u_y^2\right) + \lambda^T f(x) \tag{4.59}$$

State equation:

$$\frac{\partial H}{\partial \lambda} = \dot{x} = f(x) \tag{4.60}$$

Stationary condition:

$$\frac{\partial H}{\partial u_x} = 0 = Ru_x + \lambda_9 \tag{4.61}$$

$$\frac{\partial H}{\partial u_y} = 0 = Ru_y + \lambda_{10} \tag{4.62}$$

$$u_x = -R^{-1}\lambda_9 \qquad u_y = -R^{-1}\lambda_{10} \tag{4.63}$$

Costate equation:

$$\frac{\partial H}{\partial x} = -\dot{\lambda} \tag{4.64}$$

Expanding (4.64) gives:

$$[\dot{\lambda}_1 \quad \dot{\lambda}_2 \quad \cdots \quad \dot{\lambda}_5 \quad \dot{\lambda}_6]^T = \left[-\frac{\partial H}{\partial BA_x} \quad -\frac{\partial H}{\partial BA_y} \quad \cdots \quad -\frac{\partial H}{\partial RM_y} \quad -\frac{\partial H}{\partial RM_z}\right]^T = 0 \tag{3.65}$$

The first six elements of λ are constant. The two elements of λ that are needed in (4.63).

$$\dot{\lambda}_9 = -\frac{\partial H}{\partial V_{m_x}} = -\lambda_3 \qquad \dot{\lambda}_{10} = -\frac{\partial H}{\partial V_{m_x}} = -\lambda_4 \tag{3.66}$$

Because the derivatives in (4.66) are in terms of constants, the equations can be integrated:

$$\int_t^T \dot{\lambda}_9 dt = -\lambda_3 \int_t^T dt \qquad \int_t^T \dot{\lambda}_{19} dt = -\lambda_4 \int_t^T dt \tag{4.67}$$

$$\lambda_9(T) - \lambda_9(t) = -\lambda_3(T-t) \qquad \lambda_{10}(T) - \lambda_{10}(t) = -\lambda_4(T-t) \tag{4.68}$$

The values for the elements in λ are calculated from the boundary condition:

$$\lambda(T) = \frac{\partial \varphi}{\partial \vec{x}}\bigg|_T \tag{4.69}$$

This means that if the boundary condition is chosen independent of the missile's velocity then $\lambda_9(T)$ and $\lambda_{10}(T)$ will be zero. This leads to:

$$\lambda_9(t) = \lambda_3 t_{go} \qquad \lambda_{10}(t) = \lambda_4 t_{go} \tag{4.70}$$

The boundary condition will be used to find the values of λ_3 and λ_4. However, before it can be evaluated the final values for the missile need to be calculated. Combining (4.63) and (4.68) leads to:

$$u_x = -R^{-1}\lambda_3 t_{go} \qquad u_y = -R^{-1}\lambda_4 t_{go} \tag{4.71}$$

From the state equation:

$$\dot{V}_x = u_x = -R^{-1}\lambda_3 t_{go} \tag{4.72}$$

Integrating (4.72) leads to:

$$\int_t^T \dot{V}_{m_x} dt = -R^{-1}\lambda_3 \int_t^T (T-t)\, dt \tag{4.73}$$

$$V_{m_x}(T) - V_{m_x}(t) = -R^{-1}\lambda_3 \frac{(T-t)^2}{2} \tag{4.74}$$

$$V_{m_x}(t) = V_{m_x}(T) + R^{-1}\lambda_3 \frac{(T-t)^2}{2} \qquad V_{m_y}(t) = V_{m_y}(T) + R^{-1}\lambda_4 \frac{(T-t)^2}{2} \tag{4.75}$$

Integrating the velocity gives the position:

$$\int_t^T \dot{BM}_x dt = \int_t^T V_{m_x}(t) dt \tag{4.76}$$

$$BM_x(T) - BM_x(t) = \int_t^T \left(V_{m_x}(T) + R^{-1}\lambda_3 \frac{(T-t)^2}{2}\right) dt \tag{4.77}$$

$$BM_x(T) - BM_x(t) = V_{m_x}(T) t_{go} + R^{-1}\lambda_3 \frac{(T-t)^3}{6} \tag{4.78}$$

The missile's velocity at the final time is needed. This can be solved using (4.75).

$$BM_x(T) = BM_x(t) + \left(V_{m_x}(t) - R^{-1}\lambda_3 \frac{{t_{go}}^2}{2}\right) t_{go} + R^{-1}\lambda_3 \frac{{t_{go}}^3}{6} \tag{4.79}$$

$$BM_x(T) = BM_x(t) + V_{m_x}(t) t_{go} - R^{-1}\lambda_3 \frac{{t_{go}}^3}{3} \tag{4.80}$$

$$BM_y(T) = BM_y(t) + V_{m_y}(t) t_{go} - R^{-1}\lambda_4 \frac{{t_{go}}^3}{3} \tag{4.81}$$

Now the boundary condition can be evaluated. The boundary condition chosen for this derivation is simply the difference between the missile's current position and its desired position:

$$\varphi = \frac{1}{2} S(\overline{BM} - \overline{BM}_d)^2 \tag{4.82}$$

$$\varphi = \frac{1}{2} S\left((BM_x - BM_x d)^2 + \left(BM_y - BM_y d\right)^2\right) \tag{4.83}$$

Given that the objective is to move the defending missile between the aircraft and the attacking missile, the desired position $\overline{BM}_d$ will be on the LOS between the BA and

RM. Because they are constant, λ_3 and λ_4 can be obtained by finding their values at the final time. This is done by evaluating the derivative of (4.83) at T.

$$\lambda_3 = \frac{\partial(\varphi)}{\partial BM_x}\Big|_T = S(BM_x(T) - BM_x d(T)) \qquad \lambda_4 = \frac{\partial(\varphi)}{\partial BM_y}\Big|_T = S\big(BM_y(T) - BM_y d(T)\big) \tag{4.84}$$

Because the boundary condition is independent of the missile's velocity, $\lambda_9(T)$ and $\lambda_{10}(T)$ are zero. Next, the missile's final position can be inserted into (4.84), and λ_3 and λ_4 can be found.

$$\lambda_3 = S\left(BM_x(t) - BM_x d(T) + V_{m_x}(t)t_{go} - R^{-1}\lambda_3\frac{(t_{go})^3}{3}\right) \tag{4.85}$$

$$\lambda_3 + \frac{S}{R}\lambda_3\frac{(t_{go})^3}{3} = S\big(BM_x(t) - BM_x d(T) + V_{m_x}(t)t_{go}\big) \tag{4.86}$$

$$\lambda_3\left(1 + \frac{S}{R}\frac{(t_{go})^3}{3}\right) = S\big(BM_x(t) - BM_x d(T) + V_{m_x}(t)t_{go}\big) \tag{4.87}$$

$$\lambda_3 = \frac{S\big(BM_x(t) - BM_x d(T) + V_{m_x}(t)t_{go}\big)}{\left(1+\frac{S(t_{go})^3}{R\ \ 3}\right)} \tag{4.88}$$

Similarly:

$$\lambda_4 = \frac{S\big(BM_y(t) - BM_y d(T) + V_{m_y}(t)t_{go}\big)}{\left(1+\frac{S(t_{go})^3}{R\ \ 3}\right)} \tag{4.89}$$

This leads to the control as:

$$u_x = -\frac{S}{R}\frac{\big(BM_x(t) - BM_x d(T) + V_{m_x}(t)t_{go}\big)}{\left(1+\frac{S(t_{go})^3}{R\ \ 3}\right)}t_{go} \tag{4.90}$$

$$u_y = -\frac{S}{R}\frac{\big(BM_y(t) - BM_y d(T) + V_{m_y}(t)t_{go}\big)}{\left(1+\frac{S(t_{go})^3}{R\ \ 3}\right)}t_{go} \tag{4.91}$$

As stated previously it is desired for the missile to move between the aircraft and the incoming missile. To do this the following equations for the missile's desired position are proposed:

$$BM_x d(T) = BA_x(T) + (1 - T_s \frac{{t_{go}}^2}{TOF^2})(RM_x(T) - BA_x(T)) \quad (4.92)$$

$$BM_y d(T) = BA_y(T) + (1 - T_s \frac{{t_{go}}^2}{TOF^2})\big(RM_y(T) - BA_y(T)\big) \quad (4.93)$$

Several considerations were taken into account. First, at the end of the engagement, the BM must hit the RM. This means that as $t_{go} \rightarrow 0$ the BM's desired position should coincide with the RM's predicted position. It can clearly be seen that when t_{go} is zero, (4.92) and (4.93) reduce to:

$$BM_x d(T) = RM_x(T) \qquad \text{and} \qquad BM_y d(T) = RM_y(T) \quad (4.94)$$

The consideration is how far to start the BM's desired position away from the RM. This can be adjusted with the scaling factor (T_s). As the scaling factor is increased the BM's desired position is moved farther from the RM and closer to the aircraft. This will effectively cause the BM to react slightly slower. This reaction time can be seen in the trajectories in Fig 4.8, and Fig 4.9.

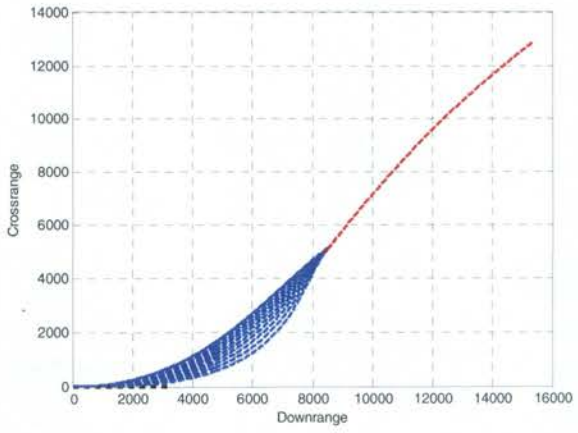

Figure 4.8 Trajectories

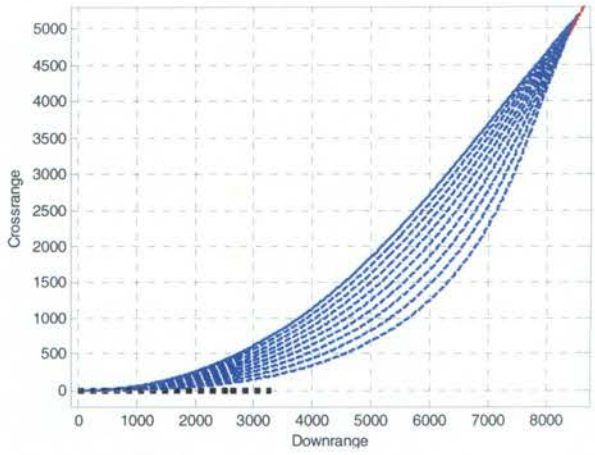

Figure 4.9 Close up Trajectories

In all of the plots for this application, the baseline is denoted by a solid line. The effect of changing Ts can be seen as it ranges from 0 to 0.9. The way that the scaling works can be seen in Fig 4.10. Essentially, the way this derivation works the target of the BM is placed on the LOS from the BA to RM. As t_{go} approaches zero, this target approaches the current position of the RM.

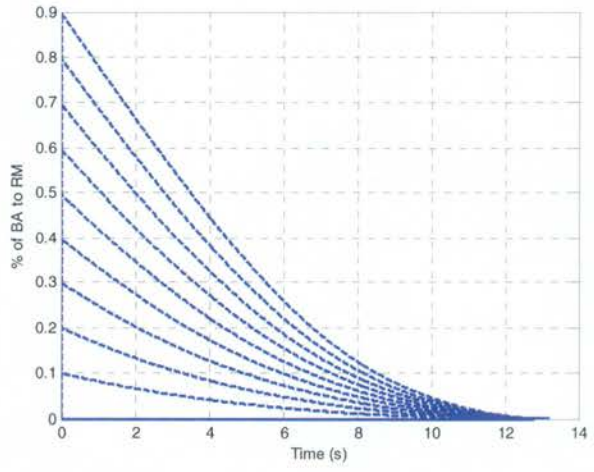

Figure 4.10 Scaling Factor Ts vs Time

In Fig. 4.10 the baseline is at 0, and the top line starting at 0.9 places the BM's target much closer to the BA. In the end, this application must outperform the baseline. The first two parameters that were considered were the miss distance and the TOF seen in Fig 4.11. In both of these parameters the baseline outperforms the new derivation. The miss distance is more than doubled as Ts increases. The TOF also increases which will cause the RM to be closer to the aircraft.

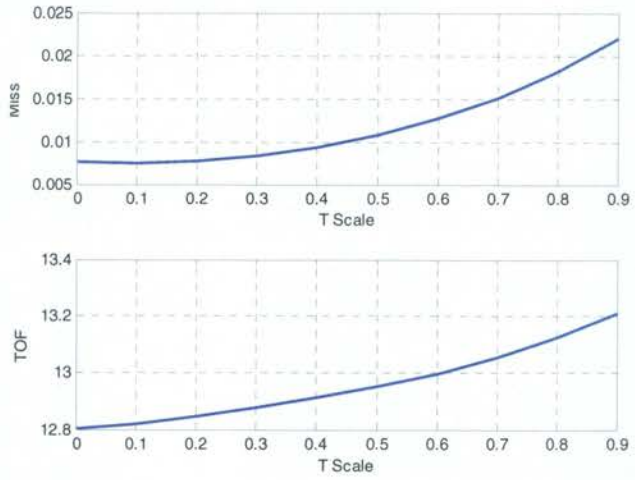

Figure 4.11 Miss Distance and TOF

In this engagement it is desirable for the BM to move between the RM and the BA. The parameter d denotes the distance from the BM to the LOS. It would be desirable to keep the BM closer to the LOS. However, it can clearly be seen that increasing Ts does not do this. Fig 4.12 shows that as Ts increases the BM drifts farther away from the LOS before it turns back toward the RM. This is because the BM reacts slower due to the lower initial weight on control.

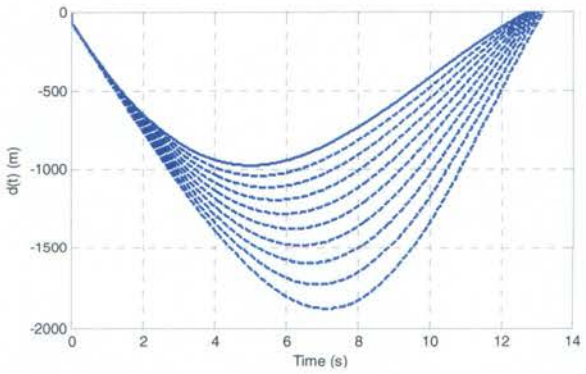

Figure 4.12 Distance from BM to LOS

These issues could be overlooked, if the control effort is significantly decreased. Two aspects of the commanded control must be considered: first, the magnitude in Fig 4.13; and second, the portion of the magnitude that is perpendicular to the velocity in Fig 4.14. This derivation gives commanded control in the x and y directions. However, it is assumed that the missile cannot control its velocity. The missile is only able to rotate by applying the portion of the commanded acceleration that is normal to the missile.

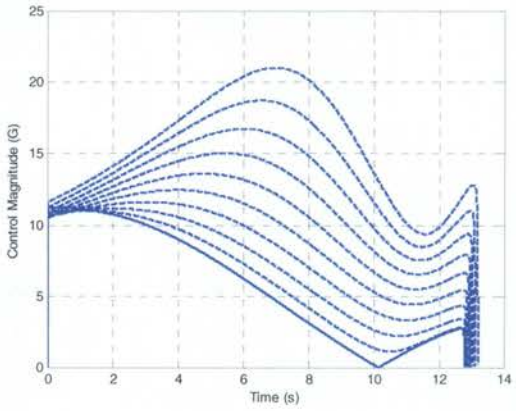

Figure 4.13 Commanded Control Magnitude

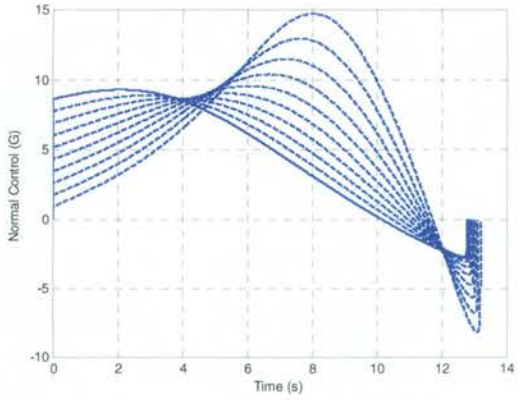

Figure 4.14 Normal Control

It can clearly be seen that as Ts increases the control effort also increases. This means that there is no benefit from using the Ts scaling. Another problem comes calculating t_{go}. In all of the simulations t_{go} was calculated using the range and range rate from the BM to the RM. There is a problem in this application, because the new target, moves between the BA and RM. This puts the target that the optimal control is shooting for closer to the initial position of the BM. This means that the BM is trying to intercept at a closer position than the predicted t_{go} is calculated for. In simulations, this lead to the commanded control trying to reduce the missile's velocity. If a missile moving at 800 m/s is told to hit a target 8,000 m away, but to take longer than 10s, it will require either a reduction in velocity or extreme weaving to burn time before hitting the target. This demonstrates the importance of t_{go} in optimal control. Using a fixed final time problem, optimal control will try to hit the target at the precise time. By contrast, a regulator problem has no need to reach its goal at a specific time. However, with a regulator problem, there is no guarantee, that the goal will be reached at a specific time.

Using this derivation does cause the BM to intercept the RM, but it does not outperform the baseline of $T_s = 0$. When T_s is zero the BM goes directly to the RM. Regardless of what metric was used, there was no performance increase from increasing T_s.

4.3. APPLICATION III

This derivation uses a coordinate frame with one of the axes along the LOS from the BA to the RM. This vector is assumed to be non-rotating because the RM uses PN. The coordinate change that rotates from the internal frame to a new frame can be expressed using two rotations, and is seen in Fig 4.15.

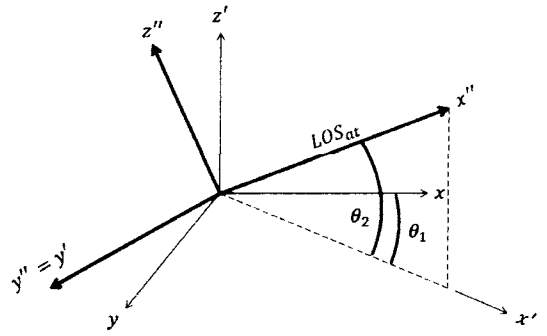

Figure 4.15 Coordinate Rotation

The LOS from the BA to the RM is denoted as LOS_{at}. The first rotation is about the inertial z axis, shown by the angle θ_1. The new coordinate system is denoted as $[x' \quad y' \quad x']$.

$$\begin{bmatrix} x' \\ y' \\ z' \end{bmatrix} = \begin{bmatrix} C_{\theta_1} & S_{\theta_1} & 0 \\ -S_{\theta_1} & C_{\theta_1} & 0 \\ 0 & 0 & 1 \end{bmatrix} \begin{bmatrix} x \\ y \\ z \end{bmatrix} \tag{4.95}$$

The second rotation is about the y' axis, shown by the angle θ_2. After this rotation, x'' will be the same direction as LOS_{at}. The transition from inertial to the new coordinate frame is:

$$\begin{bmatrix} x'' \\ y'' \\ z'' \end{bmatrix} = [T] \begin{bmatrix} x \\ y \\ z \end{bmatrix} = \begin{bmatrix} C_{\theta_2} & 0 & S_{\theta_2} \\ 0 & 1 & 0 \\ -S_{\theta_2} & 0 & C_{\theta_2} \end{bmatrix} \begin{bmatrix} C_{\theta_1} & S_{\theta_1} & 0 \\ -S_{\theta_1} & C_{\theta_1} & 0 \\ 0 & 0 & 1 \end{bmatrix} \begin{bmatrix} x \\ y \\ z \end{bmatrix} \tag{4.96}$$

Finally, it is important to note that the BA is moving. To compensate for this, relative positions and velocities will be used. Also it is assumed that the BA is moving in a straight line. The relative position and velocity of the BM will be considered in this new coordinate frame

$$\bar{x} = [BM_x \quad BM_y \quad BM_z \quad V_x \quad V_y \quad V_z]^T \tag{4.97}$$

$$\dot{\bar{x}} = f(x) = [V_x \quad V_y \quad V_z \quad u_x \quad u_y \quad u_z]^T \tag{4.98}$$

with

$$\begin{bmatrix} BM_x \\ BM_y \\ BM_z \end{bmatrix} = [T][\overline{BM}_i - \overline{BA}_i] \qquad \begin{bmatrix} V_x \\ V_y \\ V_z \end{bmatrix} = [T]\left[\bar{V}_{m_i} - \bar{V}_{a_i}\right] \tag{4.99}$$

The subscript (i) denotes the inertial frame. In this problem will assume the acceleration to be perpendicular to LOS_{at}.

$$J = \frac{1}{2}\varphi^2 + \int_{t_o}^{T} \frac{R}{2}\left(u_y^2 + u_z^2\right) dt \tag{4.100}$$

$$H = \frac{R}{2}\left(u_y^2 + u_z^2\right) + \lambda^T f(x) \tag{4.101}$$

Expanding the second term yields

$$\lambda^T f(x) = [\lambda_1 \quad \lambda_2 \quad \cdots \quad \lambda_5 \quad \lambda_6][V_x \quad V_y \quad V_z \quad u_x \quad u_y \quad u_z]^T \tag{4.102}$$

State equation:

$$\frac{\partial H}{\partial \lambda} = \dot{x} = f(x) \tag{4.103}$$

Stationary condition

$$\frac{\partial H}{\partial u_y} = 0 = Ru_y + \lambda_5 \tag{4.104}$$

$$\frac{\partial H}{\partial u_z} = 0 = Ru_z + \lambda_6 \tag{4.105}$$

$$u_y = -R^{-1}\lambda_5 \qquad u_z = -R^{-1}\lambda_6 \tag{4.106}$$

Costate equation

$$\frac{\partial H}{\partial x} = -\dot{\lambda} \tag{4.107}$$

The first three terms of λ are constant

$$[\dot{\lambda}_1 \quad \dot{\lambda}_2 \quad \dot{\lambda}_3]^T = -\left[\frac{\partial H}{\partial BM_x} \quad \frac{\partial H}{\partial BM_y} \quad \frac{\partial H}{\partial BM_z}\right]^T = 0 \tag{4.108}$$

The last two terms are functions of the second and third term

$$\dot{\lambda}_5 = -\frac{\partial H}{\partial V_{m_y}} = -\lambda_2 \qquad \dot{\lambda}_6 = -\frac{\partial H}{\partial V_{m_z}} = -\lambda_3 \tag{4.109}$$

Integrating (4.109) yields

$$\int_t^T \dot{\lambda}_5 dt = -\int_t^T \lambda_2 dt \qquad \int_t^T \dot{\lambda}_6 dt = -\int_t^T \lambda_3 dt \tag{4.110}$$

$$\lambda_5(t) = \lambda_2 t_{go} + \lambda_5(T) \qquad \lambda_6(t) = \lambda_3 t_{go} + \lambda_6(T) \tag{4.111}$$

$$t_{go} = (T - t) \tag{4.112}$$

The term t_{go} refers to the time until the end of the simulation. In this derivation it is assumed to be known. This leads to

$$u_y = -R^{-1}\left(\lambda_2 t_{go} + \lambda_5(T)\right) \tag{4.113}$$

Next we need to find the position and velocity of the BM at the final time T. The first step is to integrate the velocity.

$$\int_t^T \dot{V}_y dt = -R^{-1}\int_t^T y\, dt = -R^{-1}\int_t^T \left(\lambda_2 t_{go} + \lambda_5(T)\right) dt \tag{4.114}$$

$$V_y(T) - V_y(t) = -R^{-1}\left(\lambda_2 \frac{{t_{go}}^2}{2} + \lambda_5(T) t_{go}\right) \tag{4.115}$$

$$V_y(t) = V_y(T) + R^{-1}\left(\lambda_2 \frac{{t_{go}}^2}{2} + \lambda_5(T) t_{go}\right) \tag{4.116}$$

The position can be found by integrating the velocity.

$$\int_t^T \dot{BM}_y dt = \int_t^T V_y(t) dt \tag{4.117}$$

$$BM_y(T) - BM_y(t) = \int_t^T \left[V_y(T) + R^{-1} \left(\lambda_2 \frac{{t_{go}}^2}{2} + \lambda_5(T) t_{go} \right) \right] dt \tag{4.118}$$

$$BM_y(T) = BM_y(t) + V_y(T) t_{go} + R^{-1} \left(\lambda_2 \frac{{t_{go}}^3}{6} + \lambda_5(T) \frac{{t_{go}}^2}{2} \right) \tag{4.119}$$

Rearranging (4.115) gives

$$V_y(T) = V_y(t) - R^{-1} \left(\lambda_2 \frac{{t_{go}}^2}{2} + \lambda_5(T) t_{go} \right) \tag{4.120}$$

$$BM_y(T) = BM_y(t) + V_y(t) t_{go} - R^{-1} \left(\lambda_2 \frac{{t_{go}}^2}{2} + \lambda_5(T) t_{go} \right) t_{go} + R^{-1} \left(\lambda_2 \frac{{t_{go}}^3}{6} + \lambda_5(T) \frac{{t_{go}}^2}{2} \right) \tag{4.121}$$

$$BM_y(T) = BM_y(t) + V_y(t) t_{go} - R^{-1} \left(\lambda_2 \frac{{t_{go}}^3}{3} + \lambda_5(T) \frac{{t_{go}}^2}{2} \right) \tag{4.122}$$

The position and velocity in the z'' direction ($BM_z(T)$ and $V_z(T)$) can be found in a similar manner. The position and velocity at the final time can be used to evaluate φ. To achieve an intercept the following function is proposed

$$\varphi = \frac{1}{2} S_1 \left({BM_y}^2 + {BM_z}^2 \right) + \frac{1}{2} S_2 \left({V_y}^2 + {V_z}^2 \right) \tag{4.123}$$

The desire is for the BM to be on LOS_{at} at the final time.

$$\lambda_1(T) = -\frac{\partial \varphi}{\partial BM_x}\bigg|_T = 0 \tag{4.124}$$

$$\lambda_2(T) = -\frac{\partial \varphi}{\partial BM_y}\bigg|_T = S_1 BM_y(T) \tag{4.125}$$

$$\lambda_3(T) = -\frac{\partial \varphi}{\partial BM_z}\bigg|_T = S_1 BM_z(T) \tag{4.126}$$

$$\lambda_4(T) = -\frac{\partial \varphi}{\partial V_x}\bigg|_T = 0 \tag{4.127}$$

$$\lambda_5(T) = -\frac{\partial \varphi}{\partial V_y}\bigg|_T = S_2 V_y(T) \tag{4.128}$$

$$\lambda_6(T) = -\frac{\partial \varphi}{\partial V_z}\bigg|_T = S_2 V_z(T) \tag{4.129}$$

Using (3.122) in (3.125) leads to

$$\lambda_2(T) = S_1\left\{BM_y(t) + V_y(t)t_{go} - R^{-1}\left(\lambda_2\frac{{t_{go}}^3}{3} + \lambda_5(T)\frac{{t_{go}}^2}{2}\right)\right\} \tag{4.130}$$

Using (4.119) in (4.128) leads to

$$\lambda_5(T) = S_2\left\{V_y(t) - R^{-1}\left(\lambda_2\frac{{t_{go}}^2}{2} + \lambda_5(T)t_{go}\right)\right\} \tag{4.131}$$

Given that $\dot{\lambda}_2 = 0$, λ_2 is a constant. This means that the problem is reduced to a set of two equations and two unknowns.

$$\lambda_2 + \frac{S_1}{R}\frac{{t_{go}}^3}{3}\lambda_2 + \frac{S_1}{R}\frac{{t_{go}}^2}{2}\lambda_5(T) = S_1\{BM_y(t) + V_y(t)t_{go}\} \tag{4.132}$$

$$\lambda_5(T) + \frac{S_2}{R}t_{go}\lambda_5(T) + \frac{S_2}{R}\frac{{t_{go}}^2}{2}\lambda_2 = S_2\{V_y(t)\} \tag{4.133}$$

$$\left(1 + \frac{S_1}{R}\frac{{t_{go}}^3}{3}\right)\lambda_2 + \left(\frac{S_1}{R}\frac{{t_{go}}^2}{2}\right)\lambda_5(T) = S_1\{BM_y(t) + V_y(t)t_{go}\} \tag{4.134}$$

$$\left(1 + \frac{S_2}{R}t_{go}\right)\lambda_5(T) + \left(\frac{S_2}{R}\frac{{t_{go}}^2}{2}\right)\lambda_2 = S_2\{V_y(t)\} \tag{4.135}$$

Equations (4.134) and (4.135) can be reduced to a simplified form

$$a_1\lambda_2 + b_1\lambda_5 = c_1 \qquad a_2\lambda_2 + b_2\lambda_5 = c_2 \tag{4.136}$$

$$a_1 = 1 + \frac{S_1}{3R}{t_{go}}^3 \qquad a_2 = \frac{S_2}{2R}{t_{go}}^2 \tag{4.137}$$

$$b_1 = \frac{S_1}{2R}{t_{go}}^2 \qquad b_2 = 1 + \frac{S_2}{R}t_{go} \tag{4.138}$$

$$c_1 = S_1\{BM_y(t) + V_y(t)t_{go}\} \qquad c_2 = S_2\{V_y(t)\} \tag{4.139}$$

These equations can easily be solved using simple matrix operations.

$$\begin{bmatrix} a_1 & a_2 \\ b_1 & b_2 \end{bmatrix}\begin{bmatrix} \lambda_2 \\ \lambda_5 \end{bmatrix} = \begin{bmatrix} c_1 \\ c_2 \end{bmatrix} \qquad \begin{bmatrix} \lambda_2 \\ \lambda_5 \end{bmatrix} = \begin{bmatrix} a_1 & a_2 \\ b_1 & b_2 \end{bmatrix}^{-1}\begin{bmatrix} c_1 \\ c_2 \end{bmatrix} \tag{4.140}$$

$$\begin{bmatrix} \lambda_2 \\ \lambda_5 \end{bmatrix} = \begin{bmatrix} a_1 & a_2 \\ b_1 & b_2 \end{bmatrix}^{-1}\begin{bmatrix} c_1 \\ c_2 \end{bmatrix} = \frac{1}{a_1b_2 - a_2b_1}\begin{bmatrix} b_2 & -a_2 \\ -b_1 & a_1 \end{bmatrix}\begin{bmatrix} c_1 \\ c_2 \end{bmatrix} \tag{4.141}$$

$$\lambda_2 = \frac{b_2c_1 - a_2c_2}{a_1b_2 - a_2b_1} \qquad \lambda_5(T) = \frac{a_1c_2 - b_1c_1}{a_1b_2 - a_2b_1} \tag{4.142}$$

This gives all the information needed to calculate u_y, and u_z can be calculated in a similar way. The only change is in the equations seen in (4.139). This application showed initial success, but the final miss distance was not acceptable. The BM would miss the RM by 1-10m depending on the initial conditions. One large issue is the rotation of the coordinate system. It is assumed that the RM is using proportional navigation. This will reduce the rotation of the LOS from the BA to the RM, but it will not be zero. Even if this rotation is very small, when the distance from the RM to the BA is very large, this error becomes significant. These errors could be as high as 40 m/s. When the desired accuracy is much lower than 1m having that large of an error in velocity is unfeasible.

4.4. APPLICATION IV

Consider application III except weighting the final miss distance more. First change (4.123) to

$$\varphi = \frac{1}{2}S\left(BM_y{}^2\right) \tag{4.143}$$

This will mean that $\lambda_5(T)$ and $\lambda_6(T)$ are zero. From (4.134)

$$\lambda_2 = S\frac{\{BM_y(t) + V_y(t)t_{go}\}}{\left(1 + \frac{St_{go}{}^3}{R\ 3}\right)} \tag{4.144}$$

$$\lambda_2 = \frac{\{BM_y(t) + V_y(t)t_{go}\}}{\left(\frac{1}{S} + \frac{t_{go}{}^3}{3R}\right)} \tag{4.145}$$

Taking the limit as $S \to \infty$ leads to

$$\lambda_2 = \frac{\{BM_y(t) + V_y(t)t_{go}\}}{\left(\frac{t_{go}{}^3}{3R}\right)} \tag{4.146}$$

Leading to

$$u_y = -\frac{\{BM_y(t) + V_y(t)t_{go}\}}{\left(\frac{t_{go}{}^2}{3}\right)} \tag{4.147}$$

$$u_y = -3\left\{\frac{BM_y(t)}{{t_{go}}^2} + \frac{V_y(t)}{t_{go}}\right\} \tag{4.148}$$

Now consider the interior angle ϕ seen in Fig4.16. In the coordinate system based on the LOS from the BA to the RM, the angle can be easily expressed as

$$\sin\phi = \frac{BM_y}{R_{mt}} \tag{4.149}$$

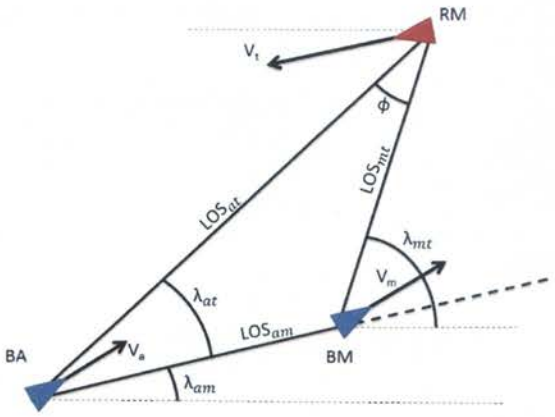

Figure 4.16 Interior Angle $\boldsymbol{\phi}$

The sine of the interior angle is the distance from the BM to the LOS, divided by the range from the BM to the RM. The range to the target can be expressed as

$$R_{mt} = V_c t_{go} \tag{4.150}$$

Assuming ϕ is small this leads to

$$\phi = \frac{BM_y}{V_c t_{go}} \tag{4.151}$$

Taking the derivative yields

$$\dot{\phi} = \frac{\dot{BM_y}}{V_c t_{go}} + \frac{BM_y}{V_c {t_{go}}^2} \tag{4.152}$$

Combining (4.152) with (4.148) yields

$$u_y = -3V_c\dot{\phi} \tag{4.153}$$

This is very close to PN seen in Equation (1.1), with a navigation constant of three, weighting a different angle. The results from this application are much more favorable. One major reason for this is that $\dot{\phi}$ can be calculated to include the rotation of the LOS between the BA and RM. This guidance law will put the BM directly on the desired LOS. Next, consider the issue seen in application II, with the difference between the commanded acceleration, and the normal acceleration. The commanded acceleration is the acceleration that optimal control tells the missile to have. The difference between these two vectors is shown by the angle θ seen in Fig 4.17. In this derivation the commanded acceleration is perpendicular to the LOS. However, the missile will not be able to provide acceleration in only this direction. In previous derivations, the portion of the commanded acceleration that is not normal to the velocity is ignored.

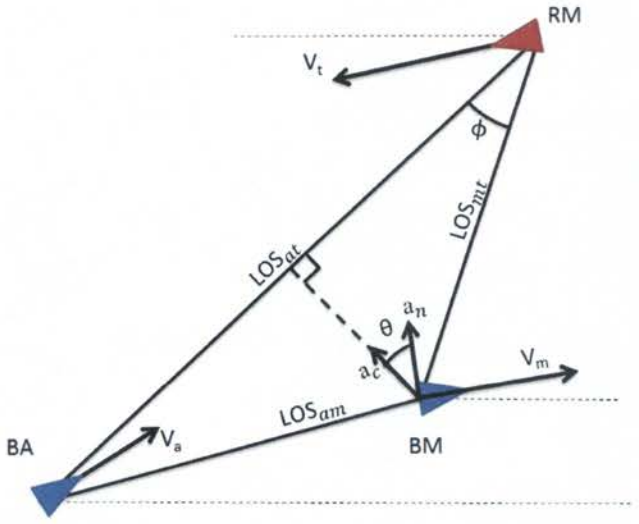

Figure 4.17 Control Angle $\boldsymbol{\theta}$

Considering that in applying optimal control to a simulation, the goal of the application should be to follow optimal control as closely as possible. In the first application this is done by forcing the optimal control derivation to be normal to the velocity. This causes major problems when moving to 3D. Therefore, rather than taking a projection of the commanded acceleration onto a vector normal to the velocity, the opposite will be done. Essentially, this is increasing the magnitude along the normal direction so that its component in the LOS frame has the same magnitude as the commanded acceleration.

$$a_n = \frac{1}{\cos\theta} a_c \tag{4.154}$$

This derivation bypasses the problem seen in the previous one due to how $\dot{\phi}$ is calculated. It can be seen from Fig. 4.18 that

$$\phi = \lambda_{at} - \lambda_{mt} \tag{4.155}$$

$$\dot{\phi} = \dot{\lambda}_{at} - \dot{\lambda}_{mt} \tag{4.156}$$

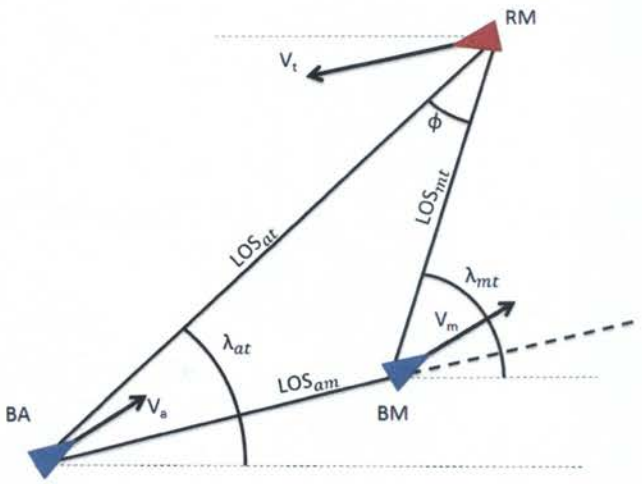

Figure 4.18 $\boldsymbol{\phi}$ Calculation

This means that $\dot{\phi}$ can compensate for the rotation of the coordinate system, because $\dot{\lambda}_{at}$ represents this rotation. The problems seen earlier do not appear in this derivation. Using the same initial conditions it has a miss distance of 3.44×10^{-7} m. The trajectory is shaped similar to what is seen in the second application. This is due to the slightly lower control effort at the beginning of the simulation. One of the objectives of applying optimal control to the Aerial Defense scenario was to reduce the initial control effort of TG. In the same engagement TG will require a much larger control effort initially. The trajectory is seen in Fig 4.19.

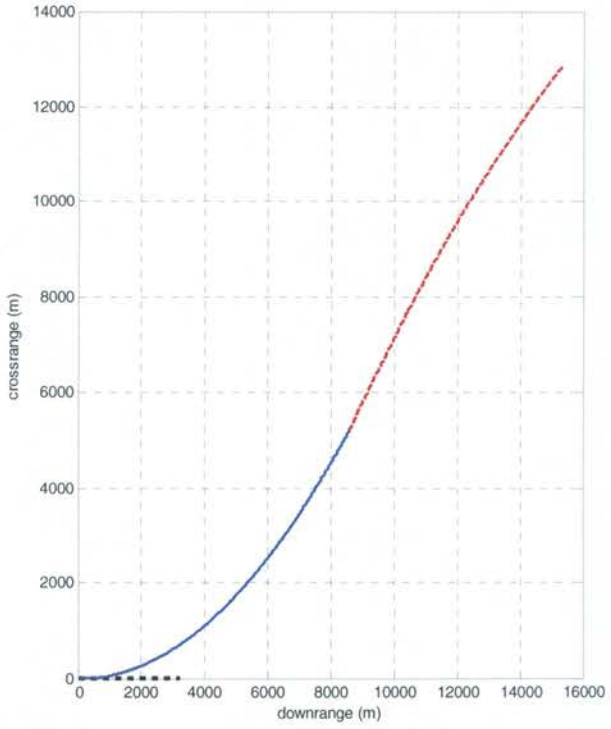

Figure 4.19 Trajectory

In this engagement the incoming missile has an initial heading error of 40^0. Despite this, the control effort is just over 10 g. There is no overreaction seen in previous derivations. The control effort is only in one direction. One problem encountered earlier was that of overshoot, when the BM crosses the LOS and must correct itself causing extra effort. It can be seen from Fig 4.20 that overshoot is not a problem, because the BM's acceleration does not change direction.

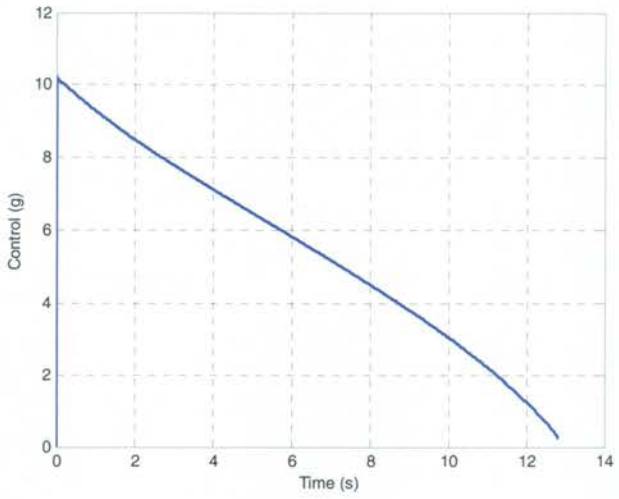

Figure 4.20 Applied Control

The distance from the BM to the LOS is seen in Fig. 4.21. This does look similar to the previous derivations, but when taken with the control there is an improvement. When the control effort is larger initially the BM will stay closer to the LOS, but it may require a correction later. This can be seen if control effort is spent counteract the initial effort. It must be kept in mind that in the optimal control formulation, there is no intermediate state weighting. TG weights σ and $\dot{\sigma}$ at the current time, and this causes the BM to reach the LOS sooner. However, this requires more effort. The formulation weights the distance to the LOS at the final time, and can be seen in Fig. 4.22.

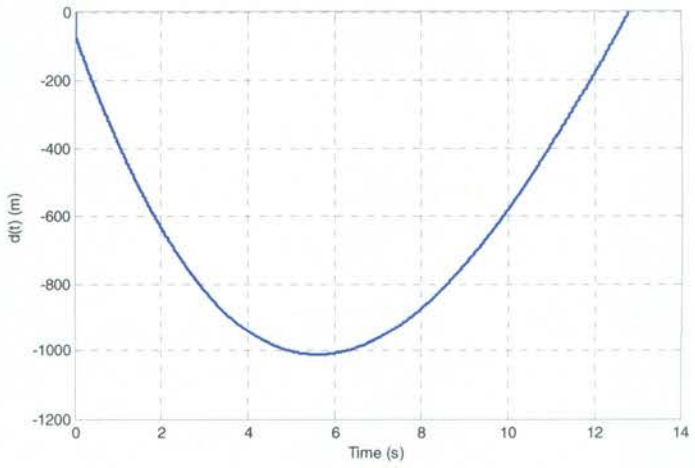

Figure 4.21 Distance to LOS

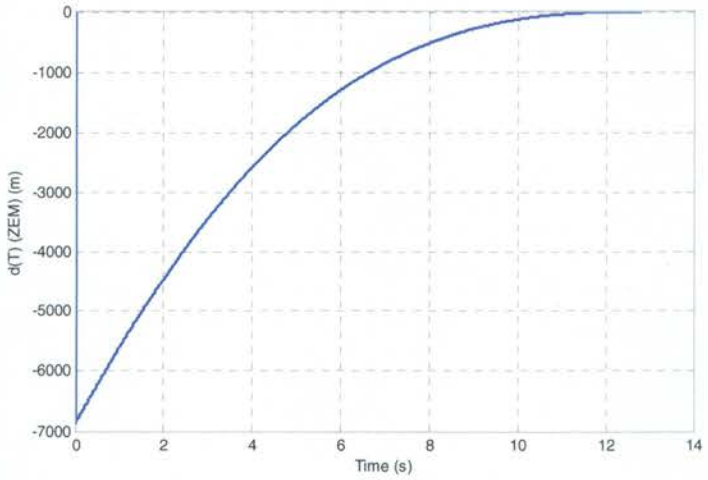

Figure 4.22 Predicted Distance to LOS

The time-to-go is known, and given the current position and velocity, the ZEM can be calculated. The ZEM is the miss distance if no effort is expended. It can be clearly seen that this is sent to zero with no overshoot.

The expansion into 3D is simpler than previous applications. The magnitude of the acceleration is the same as seen in 2D. The interior angle ϕ can be easily calculated in 3D. Representative results are shown in Fig 4.23 through Fig 4.25. The BM successfully intercepts the RM in each engagement, even when the RM starts behind the BA. The first application could not intercept the RM if it had an initial heading error larger than 65^0. For the results shown the miss distance is below 0.2m. The simulations are done in GENSIM6 courtesy of the USAF. The missiles are no longer a point mass as seen in the results from the previous applications. The velocities of the missiles are no longer constant, but change due to thrust and aerodynamic drag.

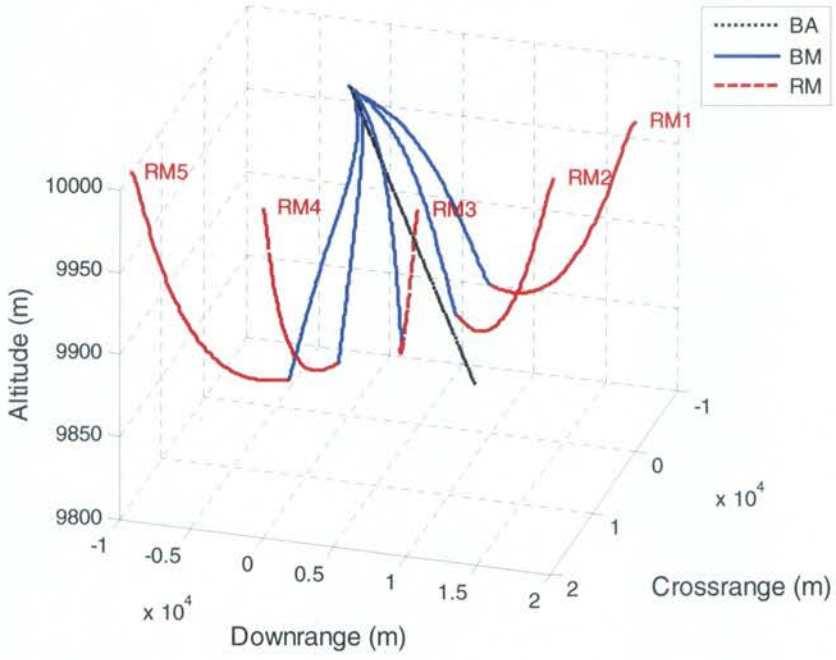

Figure 4.23 3D Trajectories

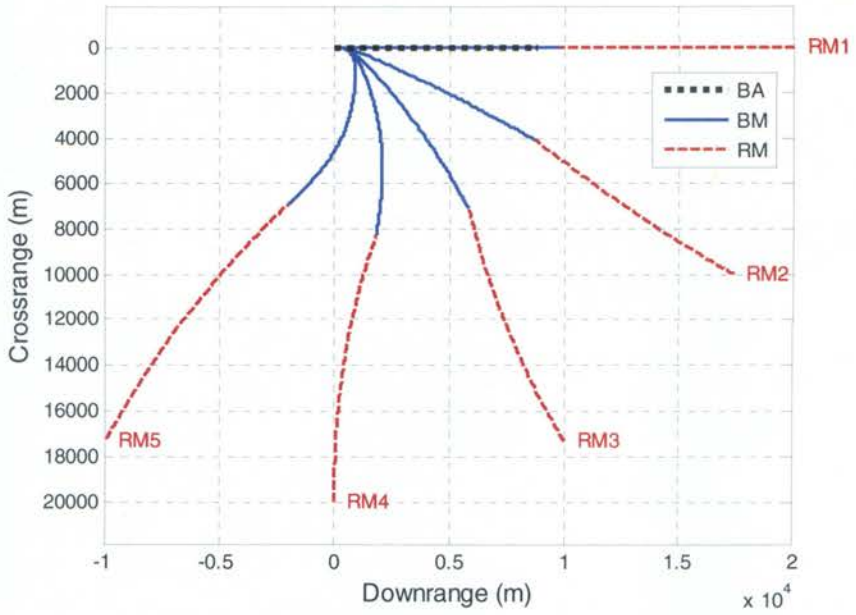

Figure 4.24 X-Y Plane Trajectories

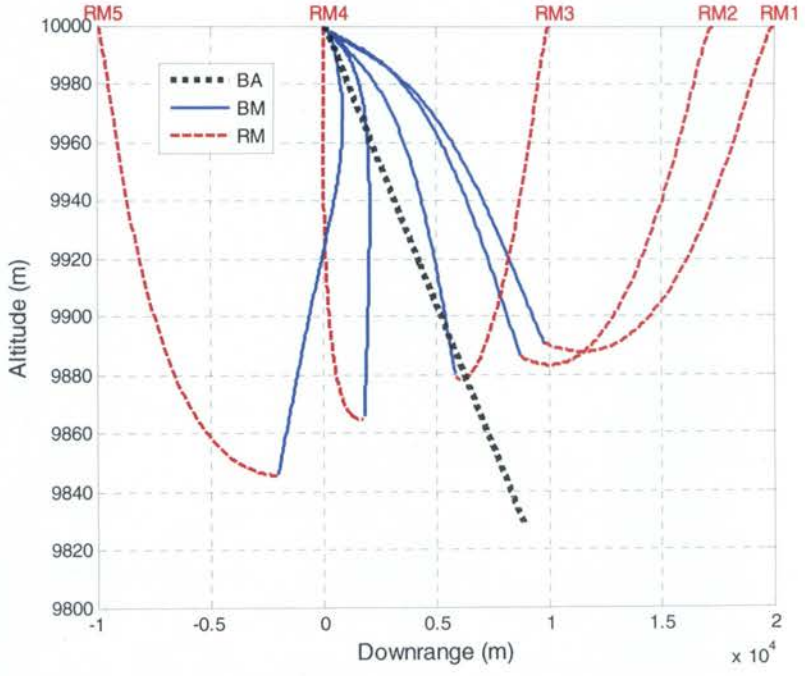

Figure 4.25 Altitude Trajectories

For a more in-depth analysis, the most extreme engagement will be examined more closely. With the RM starting behind the aircraft the BM must make a very quick turn initially. Despite this the BM is able to successfully intercept the RM. The trajectory is seen in Fig 4.26. The large initial turn is due to a large amount of control effort, seen in Fig 4.27, at the beginning of the simulation. In the simple 2D simulations the control is smooth throughout the entire simulation. This is seen only after the missiles end their thrusting phase. During the first 2.5 seconds of the simulation the BM is thrusting, and this is clearly seen in Fig. 4.28. After this short thrusting period the missile's velocity slows down due to drag. The incoming missile's velocity behaves in a similar way.

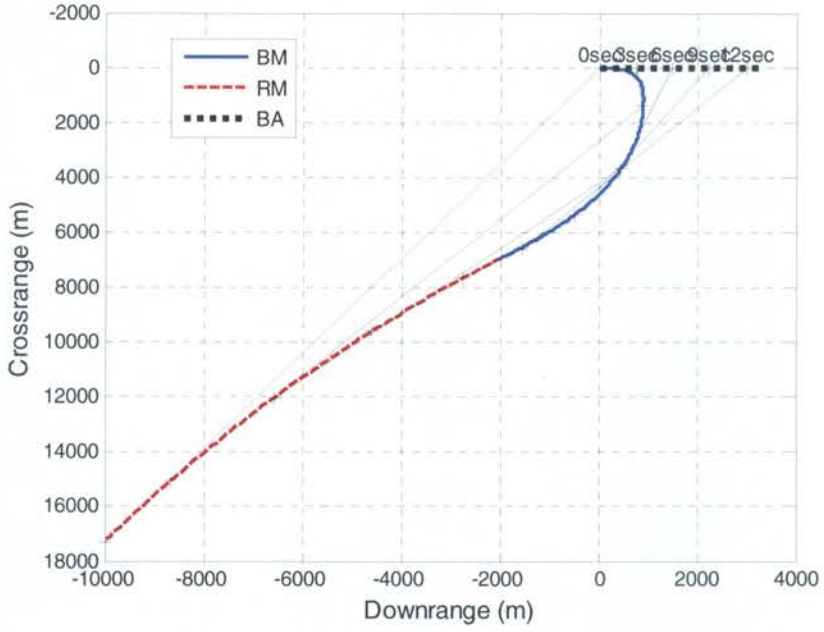

Figure 4.26 Sample Trajectory

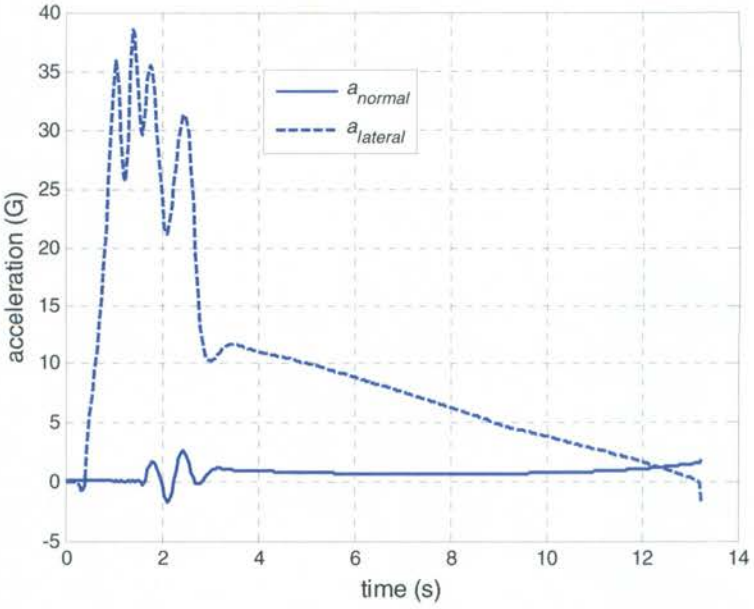

Figure 4.27 Sample Control

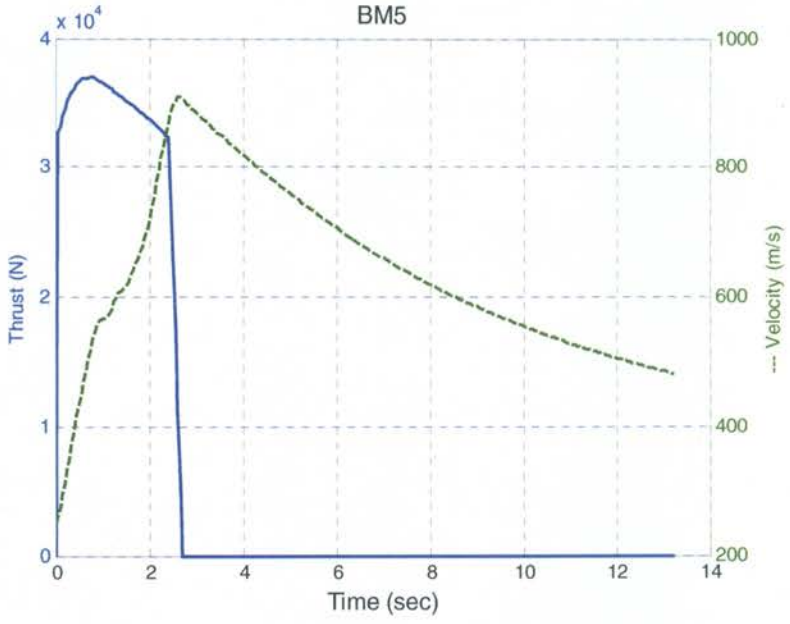

Figure 4.28 BM Velocity

5. CONCLUSIONS

The basic goal of this paper is to apply optimal control to the Aerial Defense engagement. This was done with four applications of the optimal control derivation. The first applications are a more direct using σ similar to what is seen in TG. TG weights the angle σ so this was put into optimal control by using σ in the final state constraint. This derivation works well initially, but requirs a hyperbolic weight on control, and a scaling on the t_{go}. With these additions the miss distance was decreased to acceptable levels. The goal seemed to be achieved, because the initial control effort was decreased from TG. However, there was a major problem when applying the derivation to 6-DOF. Essentially, the differential equation for the additional Lagrange multiplier is not solvable. This means that no expression can be found for the additional control term. Without this the 6-DOF derivation does not work.

The second derivation uses an inertial expression for the control vector. It is broken up into its x and y components. This will bypass the problem seen when applying the first derivation to 6-DOF. This causes a new problem dealing with the fact that the missile cannot control its velocity. To get around this problem, the axial acceleration is ignored. In the end the second derivation fails to outperform the baseline. Using the entire engagement does not provide any benefits over merely having the BM intercept the RM. The optimal route for the second derivation is to set Ts to zero, which ignores any information from the aircraft.

The third derivation weights the distance to the LOS rather than σ. A new coordinate system is used to simplify the optimal control expressions. Both position and velocity relative to the LOS are used. This was done in an attempt to prevent overshoot. In the end the rotation of the coordinate system causes enough error to increase the miss distance beyond acceptable levels.

The final derivation is similar to the third, but takes the limit as the final state weight goes to infinity. This changes the problem from free final state to fixed final state. Only the final position is weighted, which simplifies the control expression. Taking the limit allows it to be simplified even further. The final expression is similar to PN, and

proves to have very good results. The problem seen with the coordinate system rotation is accounted for in the calculation of $\dot{\phi}$. The control effort is low, while still keeping the miss distance small. This derivation uses the engagement geometry in optimal control to have the BM intercept the RM.

BIBLIOGRAPHY

[1] Machol, R. E., Tanner, Jr., W. P. and S. N. Alexander, *System Engineering Handbook*, Chap. 19 Guidance, R. E. Howe, McGraw-Hill Book Company, 1965.

[2]Goodstein, R. "Guidance Law Applicability for Missile Closing." AGARD *Lecture series No. 52: Guidance and Control of Tactical Missiles.* London: Technical Editing and Reproduction Ltd Hartford House, 1972.

[3]Zarchan, P. *Tactical and Strategic Missile Guidance.* 2nd Ed. Vol. 157. Washington DC: American Institute of Aeronautics and Astronautics, 1994.

[4]Dorr and Bishop 1996

[6]Robb, M.C., Tsourdos, A., and White, B.A., "Earliest Intercept Line Guidance Using a Game Theory Approach," *Proceedings of AIAA GNC Conference*, AIAA 2006-6216 , Colorado, 2006.

[7]Boyell, R.L. "Defending a Moving Terger Against Missile or Torpedo Attack," *IEEE Transactions on Aerospace and Electronic Systems,* vol. AES-13, No. 3, pp. 321, 1977.

[8]Rusnak, I., "Guidance laws in defense against missile attack," *Proceedings of the IEEE 25th Convention of Electrical and Electronics Engineers in Israel,* (IEEEI 2008), pp.90-94, 2008

[9]Perelman, Andery and Shima, Tal, "Cooperatuve Differential Games Strategies for Active Aircraft Protection from a Homing Missile," *AIAA Guidance, Navigation, and Control Conference*, AIAA 2010-7878, 2010.

[10]Ratnoo, Ashwini and Shima, Tal, "Line of Sight Guidance for Defending an Aircraft," *AIAA Guidance, Navigation, and Control Conference*, AIAA 2010-7877, 2010.

[11]Yamasaki, Takeshi, and Balakrishnan, S. N. "Triangle Guidance for Aerial Defence," *AIAA Guidance, Navigation, and Control Conference*, AIAA 2010-7876, Toronto, Canada, 2010.

[12]Chima, Tal, and Shaferman, Vitaly, "Cooperative Multiple Model Adaptive Guidance for an aircraft Defending Missile," *AIAA Guidance, Navigation, and Control Conference*, AIAA 2010-8320.

[13]Yamasaki, Takeshi, and Balakrishnan, S. N. "A-CLOS," *AIAA Guidance, Navigation, and Control Conference*,

[14] Lewis, Frank and Syrmos, Vassilis, Optimal Control, second edition, Wiley-Interscience Publication, 1995

[15]Bryson, A.E., Jr. and Ho, Y.-C., Applied Optimal Control,-Optimization, Estimation, and Control, 1975 (Hemisphere Publishing Corporation, New York).

[16]Rusnak, I., "Guidance laws in defense against missile attack," *IEEE Convention of Electircal and Electronics Engineers in Israel,* (IEEEI 2008)

[17]Robb, M.C., White, B.A., Tsourdos, A. and Rulloda, D., "Reachability guidance: a novel concept to improve mid-course guidance," *AIAA GNC Conference,* AIAA2005-417, 2004.

[18]Shima, T., M. Idan, and O. M. Golan, "Sliding-Mode Control for Integrated missile Autopilot Guidance," *Journal of Guidance, Control and Dynamics,* Vol. 9, No. 2, pp250-260, 2006.

[19]Zipfel, P., *Modeling and Simulation of Aerospace Vehicle Dynamics, Second Edition,* AIAA Education Series, AIAA, 2007

[20]Harl,N., Balakrishnan,S.N., and Phillips, C., "Sliding Mode Integrated Missile Guidance and Control," *Proceedings of AIAA GNC Conference*, AIAA 2010-7741, Toronto, 2010.

VITA

Andrew John Friedrichs was born on September 18, 1986. In May 2009 he received his BS Aerospace Engineering from the Missouri University of Science and Technology. He received a Chancellors fellowship to pursue graduate studies at the same university. In the spring of 2010 he presented a paper to Missouri Space Grant on sliding mode reentry. He was awarded a teaching fellowship and taught Introduction to Engineering Design for a total of four semesters. In the fall of 2010 he began a research fellowship, funded by the USAF, under Dr. Balakrishnan. This research led to the development of Optimal Triangle Guidance, and he was one of 10 graduate students to present the national AIAA conference in January of 2012. In August 2012, he received his MS degree in Aerospace Engineering from the Missouri University of Science and Technology.